Measurements of the Kinetics and Transport Properties of Contaminants Released from Polymeric Sources in Space and the Effects on Collecting Surfaces

by

E. A. Zeiner
Aerojet ElectroSystems Company

Abstract

Under a recent USAF contract, AESC performed measurements on the emission kinetics, reemission kinetics, and surface transport properties of the contaminants (CVCM) which are released by polymeric sources in space. In addition to these mass transfer properties, measurements were made on the optical effects these contaminants had on receptors upon which they deposit.

1. INTRODUCTION

The testing work done at AESC in support of the USAF Satellite Contamination Program covered five basic testing areas. These tasks were: 1) source emission kinetics, 2) receptor reemission kinetics, 3) surface transport properties, 4) laser induced kinetics, and 5) contaminated receptor optical effects. The laser kinetics work is not covered in this report due to classification.

Two primary test facilities were employed in which to make the necessary measurements. For the mass transfer measurements covering the first three of the above tests, the AESC Molecular Kinetics Test Facility (Molekit) was used. Its primary instrument consists of an array of four quartz crystal microbalances (QCMs) positioned directly in front of the source. The contamination effects measurements were made in the AESC Surface Materials Effects Facility (SMEF). For this effort, the SMEF used an integrating sphere to measure changes in the spectral reflectance and transmittance on five typical receptors which were contaminated by the source materials and then irradiated with ultraviolet light.

In addition to obtaining the source material properties themselves, a substantial amount of the work was directed at developing the test techniques to facilitate both the precision and the speed of the measurements. This is particularly true for the mass transfer tests in the Molekit. While the necessity of applying QCMs to evaluate reemission kinetics from contaminated surfaces is clear, it is not so clear that these same instruments can be used to evaluate source emission kinetics. This indirect technique, identified as cryogenic QCM thermogravimetric analysis (CQ/TGA) requires considerable knowledge of the test configuration and rigorous temperature control of all components of the facility. Since free molecule flow conditions are maintained, the only transport property evaluated is the surface capture coefficient.

This is primarily the probability that an incident molecule will become thermally accommodated upon collision with the surface of the receptor. Two typical source materials were studied; one, RTV-566 (0.2% catalyst), was studied fairly completely.

In the SMEF, reflectance measurements were made with about 1000 Å of volatile condensible materials (VCMs) from RTV-566 adhesive and after thirty-six hours of irradiation with thirty equivalent ultraviolet suns (30 EUVs) of light at 1236 Å. However, the data reduction was not completed in time to include the results in this report.

Significant characteristics of the Molekit and the SMEF are that their internal configurations and procedures were developed by direct application of the system contamination equations. This insures that the flux coupling geometry of the chamber components can be rigorously accounted for in evaluating material properties.

2. VCM MASS TRANSFER TESTS

This section covers a brief description of the Molekit and the three areas of testing performed in it. Included is an outline of the QCM calibration techniques necessary for CQ/TGA of source materials kinetics.

2.1 AESC Molecular Kinetics Test Facility (Molekit)

This facility is displayed in Figure 1. It is a vertical cylinder 2-1/2 feet high and 2-1/2 feet in diameter. The outer shell contains a complete cryogenic shroud which is maintained at LN_2 temperatures in all tests. The basic instrumentation consists of a coplanar array of four QCMs which can be positioned from about 1/2 inch to 6 inches in front of the source holder. This array can be held at any temperature from -170°C to 150°C with better than ±1/2°C accuracy. The source holder supports a 1-inch-diameter source specimen and it can be maintained from -170°C to about 140°C with the present temperature controllers. All internal cryogenic and LN_2 lines are covered with foil to minimize radiation coupling. The entire Molekit (without sources) can be baked out in vacuum at up to 150°C. The Molekit is fore pumped with 4 sorption pumps and will maintain near 10^{-8} torr with a 500 liter/sec ion pump; thus no pumps using hydraulic lubrication or diffusion oil are used which minimizes spurious gas loads. Temperatures are monitored throughout the Molekit at 15 locations.

All data is automatically acquired once the test starts using the HP-3050A automatic data acquisition system depicted on the control panel in Figure 2. Data is sampled at precisely programmed intervals, stored on magnetic tape, printed out, and plotted for real time "quick-look" analysis and system diagnosis. This is also true of the SMEF.

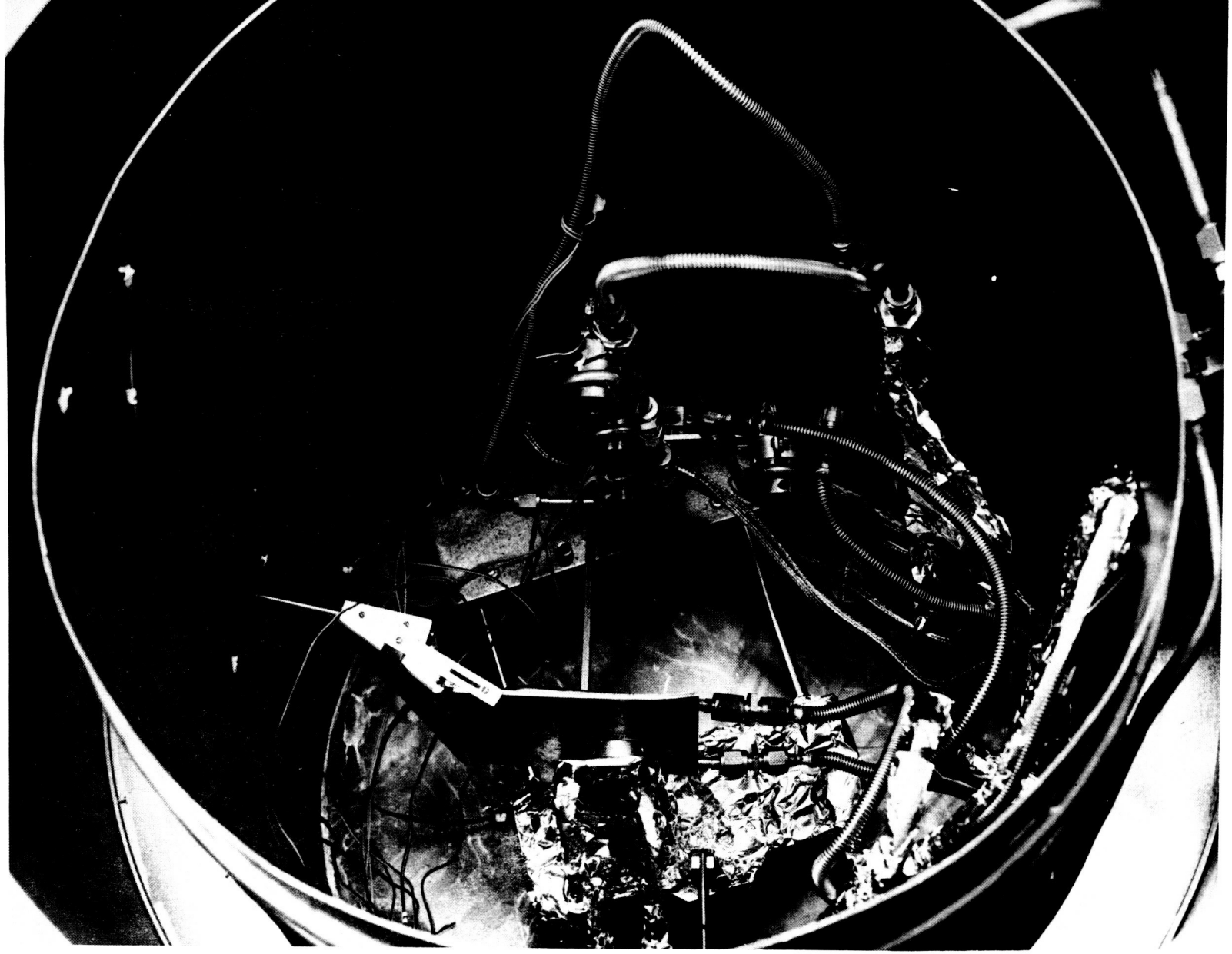

Figure 1. The Molecular Kinetics Test Facility

Figure 2. Control Console with HP-3050A Automatic Data Acquisition System

2.2 QCM Calibration Procedures

Prior to performing the source kinetics tests using the indirect CQ/TGA technique, calibration of the QCMs is necessary due to a significant variation in the beat frequency of these units in response to the thermal radiation flux from the hot source. To do this, a "dummy" source is mounted on the support which duplicates the emissivity of the polymeric source, but doesn't emit VCM. Baked-out marble discs were used for these calibration tests. The dummy source is then cycled through a complete test sequence, and the transient beat frequency of each QCM is recorded long enough until a steady output is obtained for each unit. The response for a 2-inch separation between the source and the QCM array is plotted for two heating steps of the source in Figure 3. While the basic mode of response is the same for each QCM, there are significant variations for any given unit, hence the calibration curve is necessary for each individual QCM unit.

This data is stored on tape and is then subtracted from the contamination data, thus correcting the raw data for the QCM transient thermal response.

2.3 Source Kinetics Tests Procedures

A direct and reliable method for determining exact source kinetic properties is to suspend the source specimen on a vacuum microbalance in-situ and maintain a constant temperature until the outgassing becomes negligible. This is classical isothermal TGA. The data that is measured directly is the weight remaining, M_s, in the source. The mass loss rate $\dot{M}_s$, is a second variable which can be obtained from the slope of the M_s versus time profile. For an isothermal first-order rate process, Figure 4 represents a typical M_s time profile for a source, which contains 2 active components. One important characteristic implicit on Figure 4 is that the activity or volatility of the two active components is sufficiently different so that by the time the high volatile

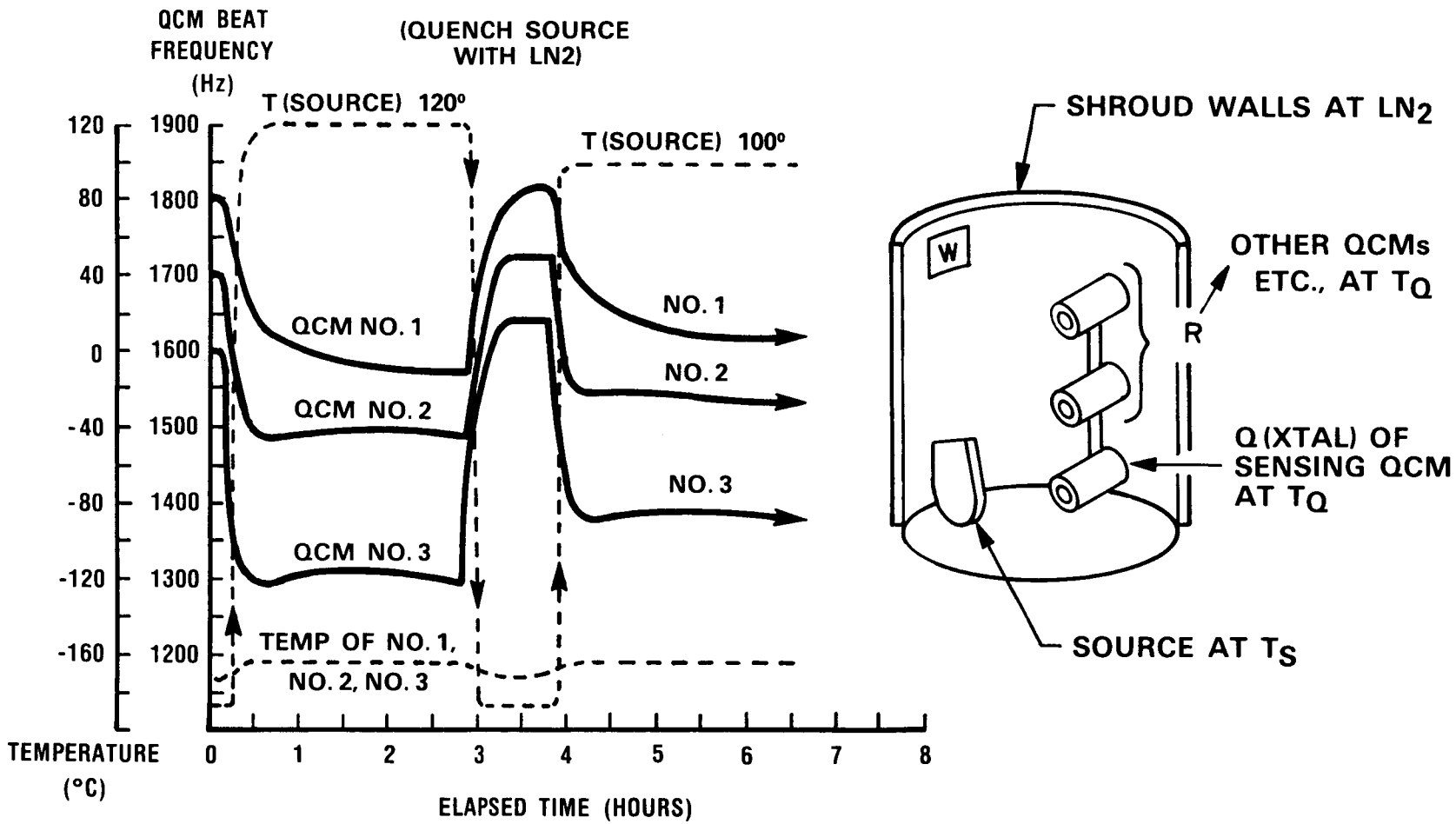

AEROJET ELECTROSYSTEMS COMPANY

Figure 3. Transient Frequency Response of a QCM Held at -170°C to Step Heating by a Source Between -180°C and 120°C

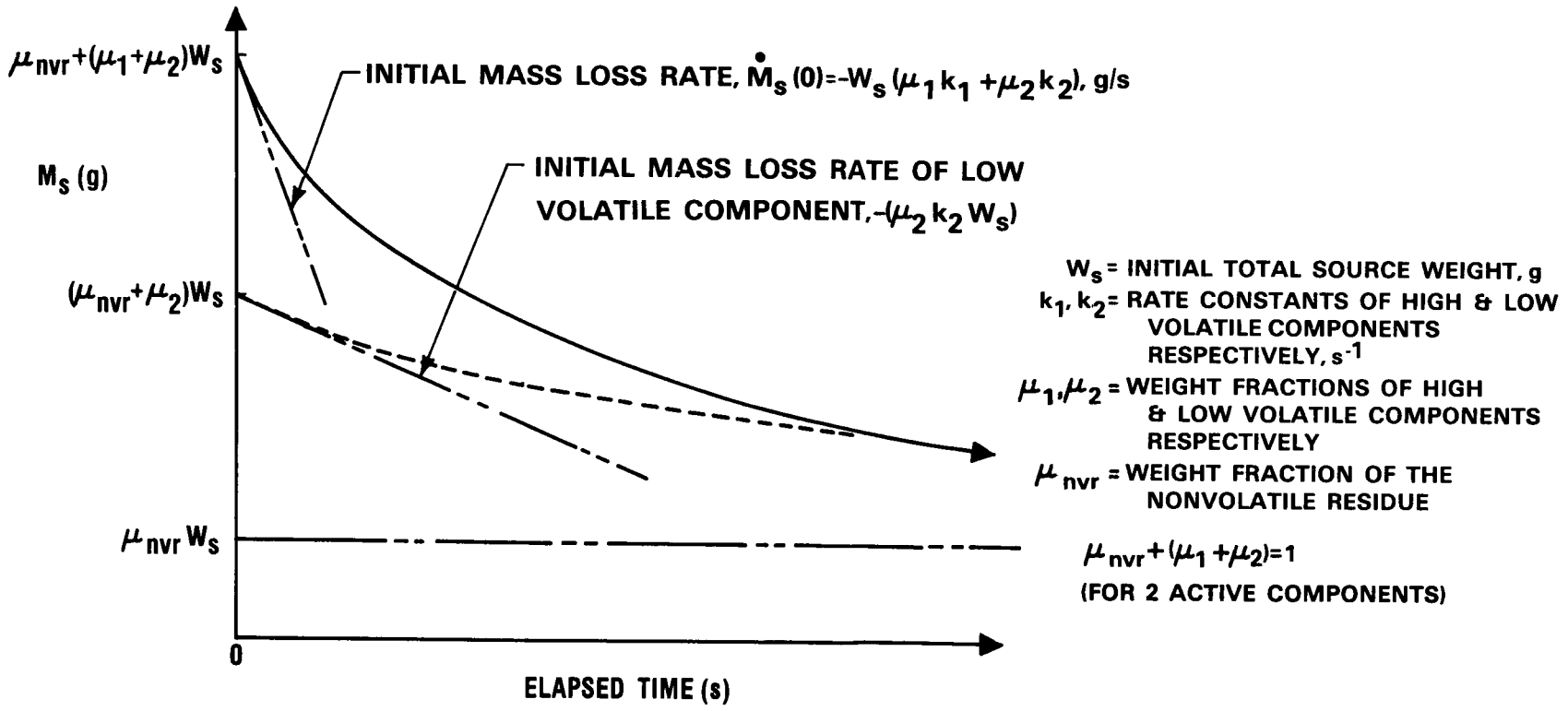

Figure 4. Source Kinetics Parameters Applied to a Typical 2 Component Polymer During Isothermal TGA

component (HVC, #1) is depleted, the low volatile component (LVC #2) is still active enough to exhibit measurable changes to the deposition rate. When this is true, then the data is "tail-of-the-test" data, where changes are due to the LVC only. Thus, the value of the rate constant of the LVC can be determined from the slope and weight fraction by extrapolating to the origin. The weight fraction of the non-volatile residue (μ_{nvr}) must also be known. The initial total mass loss rate together with any other point where both components are active, will give the weight fraction and the rate constant of the HVC. Independent measurements of the total initial source weight and the non-volatile residue mass fraction are required. More than two components can be evaluated with this general procedure provided the activity of the components is widely separated.

For source kinetic processes which are rate processes greater than first order processes, a completely analogous procedure applies. When more general kinetics such as surface-mediated diffusion is present, a somewhat similar procedure is used, but the process requires fitting the entire mass remaining profile to obtain the diffusion parameters. In general, this requires a polynomial regression analysis on a computer instead of the simple graphical procedures permissible in the case of first order kinetics.

For most real space qualified materials, the volatility of the active VCM components is quite low by design, hence a very long test time is required to perform the isothermal TGA using vacuum weighing systems with methods just described. This problem is further complicated by the mass sensitivity limitations of an in situ vacuum microbalance system if it is used. Measurements of this kind to obtain source kinetics were studied but were not performed.

Another method is available for measuring source kinetics. This technique uses QCMs which are maintained at LN_2 temperatures so that the VCM remission is negligible. The source temperature is maintained

at a constant value so that this method is designated isothermal cryogenic QCM TGA (CQ/TGA). Its principle shortcoming is that the source directional mass loss distribution must be known. This distribution can be measured by an array of QCMs such as is employed in the Molekit. Its main advantages over the isothermal TGA are that the QCMs are extremely sensitive being able to detect nanograms of mass loss from the source, and that it can be applied to the most general complex source configurations used on typical satellite systems. CQ/TGA, being at the present a state-of-the-art isothermal procedure, requires about 48 hours including set-up time to evaluate a typical low volatile space qualified source. By virtue of CQ/TGA high sensitivity, it requires considerably less time than conventional isothermal TGA with vacuum balances. While dynamic TGA is the most rapid of all testing procedures, it is limited to the source configurations it can handle and at present it can only characterize sources in terms of rate ordered processes at relatively high temperatures. This is probably valid at temperatures in excess of 200°C for most source materials which are applied as relatively thin coatings. However, at near ambient source temperatures, even with thin coatings, much of the mass loss kinetics is probably diffusion limited, and isothermal methods are again necessary.

To reliably obtain the kinetic parameters of the source materials, it is necessary to accurately model the AESC Molekit configuration and then adjust the geometry of the internal components to establish the optimum configuration for testing. The Molekit can be modeled as a four-node system. These nodes are the crystal of the sensing QCM (Q), the cases of all four QCMs and their support structure (R), the source and its holder (S), and the Molekit shroud walls (W).

The basic equation for CQ/TGA to evaluate source kinetics is, assuming the source to emit diffusely(cosine distribution),

$$\dot{M}_Q = -F_{SQ}\dot{M}_S \qquad (1)$$

where

$\dot{M}_Q$ = total mass deposition rate on the QCM, g/s

$\dot{M}_s$ = total mass loss rate from the source (a negative value), g/s

F_{SQ} = diffuse geometric view factor from the source to the QCM crystal

If an explicit functional form of $\dot{M}_s$ is known, which is integrable, equation (1) can be integrated to give the CQ/TGA equation for source kinetic testing. If it is assumed that the most likely source process is the exponential first order process, then two independent equations(M_Q and $\dot{M}_Q$) will characterize the CQ/TGA procedures allowing the simultaneous evaluation of 2 independent material properties. Thus a two component source is indicated which exhibits first order source emission. The QCM deposition expression assuming an initially clean QCM and a diffuse source, becomes

$$\left.\begin{aligned} M_Q &= F_{SQ}\, W_S \left[(\mu_1 + \mu_2) - \left(\mu_1 e^{-k_1 t} \right) - \left(\mu_2 e^{-k_2 t} \right) \right] \\ \dot{M}_Q &= F_{SQ}\, W_S \left(\mu_1 k_1 e^{-k_1 t} + \mu_2 k_2 e^{-k_2 t} \right) \end{aligned}\right\} \qquad (2)$$

where

M_Q = mass on the QCM, g

W_S = total weight of source material before testing, g

μ_1, μ_2 = weight fractions in the source of the two source components

k_1, k_2 = rate constants at T_s, for the two source components, s^{-1}

The QCM is a "beat" frequency which is directly proportioned to the deposited mass. Analytically, this is expressed as

$$\left.\begin{aligned} M_Q &= A_Q C_Q (f - f_o) \quad , \quad g \\ \dot{M}_Q &= Q_Q C_Q \dot{f} \quad , \quad g/s \end{aligned}\right\} \tag{3}$$

where

A_Q = 0.316 cm^2, the active area of the QCM crystal

C_Q = 4.43×10^{-9} $g\text{-}cm^{-2}$ - Hz; the mass sensitivity constant for these QCMs

f = instantaneous beat frequency of the QCM, Hz and

f_o = initial baseline (clean) beat frequency of the QCM, Hz.

Combining equations (2) and (3) expresses the four source kinetic properties (μ_1, μ_2, k_1, k_2) in terms of two isothermal observables, (f,$\dot{f}$).

$$(\mu_1 + \mu_2) - \left(\mu_1 e^{-k_1 t} + \mu_2 e^{-k_2 t}\right) = C(f-f_o)$$

$$\left(\mu_1 k_1 e^{-k_1 t} + \mu_2 k_2 e^{-k_2 t}\right) = C\dot{f}$$

where

$$C = \left(\frac{A_Q C_Q}{F_{sq} M_{so}} \right) \text{ Hz}^{-1} \text{ and}$$

$\dot{f}$ = instantaneous rate of change in beat frequency, $\text{Hz} \cdot \text{s}^{-1}$.

A basic requirement to use this method (and any other multi-component technique such as dynamic TGA) is that the two active components are sufficiently different in their kinetic activity that the high volatile component (HVC or μ_1) is completely depleted from the source while the lower volatile component (MVC, or μ_2) is still being released in significant amounts. The basic procedure allows the tests to run long enough for the high volatile component to be completely depleted so that the "tail" of the test can be analyzed when only the lower volatile material is still outgassing. Once the two properties of the low volatile have been determined, earlier data where both species are active can be used to compute the values of μ_1 and k_1. This "Tail of the Test" procedure can be used to analyze sources with more than two components provided that the rate constants of the components are significantly different. The method simply starts at the end of the test and works backwards to the beginning solving for the components of each successive active component.

It has been shown (Dow Corning, Ball Brothers, etc.[2]) that many organic polymers of the type currently being used in satellite applications do indeed exhibit a highly volatile component which off-gasses relatively rapidly (about 10 to 15 hours for $T_s \approx 125°C$) followed by a very slowly emitting component which exhibits a nearly constant deposition rate when the high volatile component has been depleted. Figure 5 presents a representative example of such a typical two component polymer, and identifies the significant observables during a cryogenic QCM thermogravimetry test.

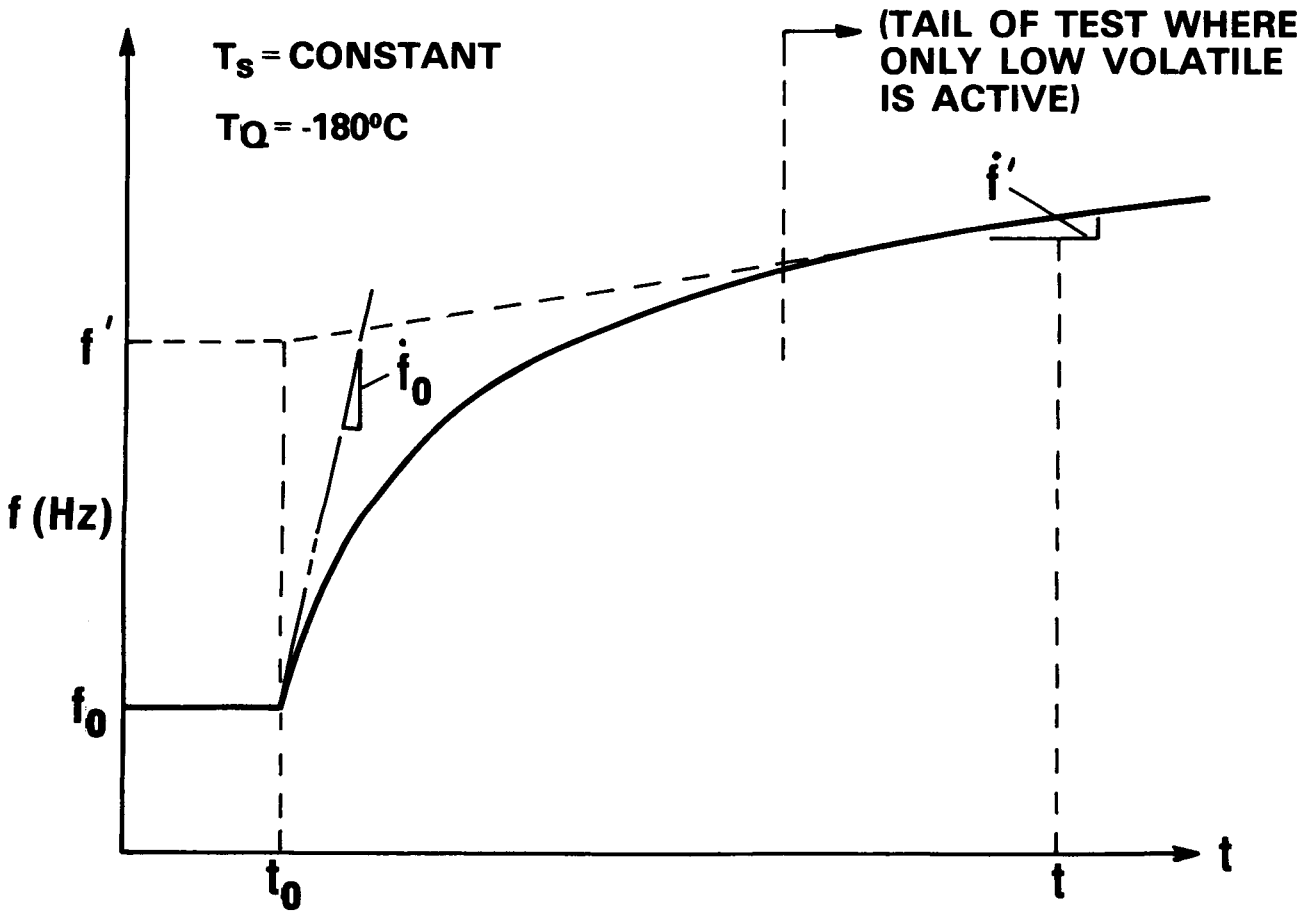

Figure 5. Typical Isothermal QCM Thermogravimetric Data for a Two Component Polymeric Source

If sufficient test time is allowed, the high volatile component is depleted and, assuming a constant outgassing rate for the low volatile component simplified graphical relationships develop as follows

$$\mu_2 k_2 = C\dot{f}'$$

$$\mu_1' k_1 = C(\dot{f}_o - \dot{f}') \tag{4}$$

$$\mu_1 = C(f' - f_o).$$

If the constant slope, $\dot{f}'$, is projected to the starting time of the test, then the $(f' - f_o)$ measures the mass of the high volatile component which is present in the source sample during the test. This will always be slightly less than the actual mass fraction due to undetected losses which occur during the pumpdown and initial test procedures in vacuum prior to the start of deposition. The rate constant for the high volatile component is simply

$$k_1 = \left(\frac{\dot{f}_o - \dot{f}'}{f' - f_o} \right). \tag{5}$$

Of course the QCM calibration data must be applied to the raw test data to obtain the curve shown in Figure 5.

One limitation in these types of tests is that the source outgassing component which is the most volatile begins leaving the source as soon as the chamber is pumped. Thus, it is clear, that the source should be quenched with LN_2 as soon as possible after starting the pumpdown to preserve as much of these high volatiles as possible. There are

two constraints to this procedure. The first is that if the source is chilled too fast, water vapor can condense on the cold sources, which can significantly change the initial mass loss characteristics. Secondly, if the chamber walls are not kept continually colder than the source, any condensibles on the walls (from previous tests, etc.) can be readily transferred to the source. Thus, the overall constraint is how fast the entire Molekit system can be brought to cryogenic temperatures.

The Molekit at present accomplishes this in about ten minutes using a sequence of aspirators and sorption pumps for the rough pumping. The optimum pressures at which the cryogen is admitted into each subsystem of the facility has been experimentally optimized so that it is estimated only about 5% of the high volatile is lost.

2.4 Source Kinetics Test Results

During the source kinetics testing phase of the program, two source materials were evaluated. A single source kinetics test was run on DC 92-007 at 100°C and three tests were run on RTV-566 at 40°C, 70°C and 120°C. The raw data is presented as it was obtained on the data acquisition plotter during the tests. The QCM calibration has not been applied to this raw data. The QCM array during the DC 92-007 test is 15.24 cm from the source.

The outgassing characteristics of DC 92-007 at 100°C are presented in Figure 6. The accumulation on 3 QCMs is shown. The first QCM is concentric with the source while the other two are coplanar with the on-axis QCM and make angles of about 26° and 53° with that axis. The ratio of the deposition on the first two QCMs clearly indicates Lambertian (diffuse) emission from the source. The outermost QCM gives value about 50% greater than diffuse, but subsequent tests have shown this QCM to be faulty. It has since been removed from the Molekit. Diffuse

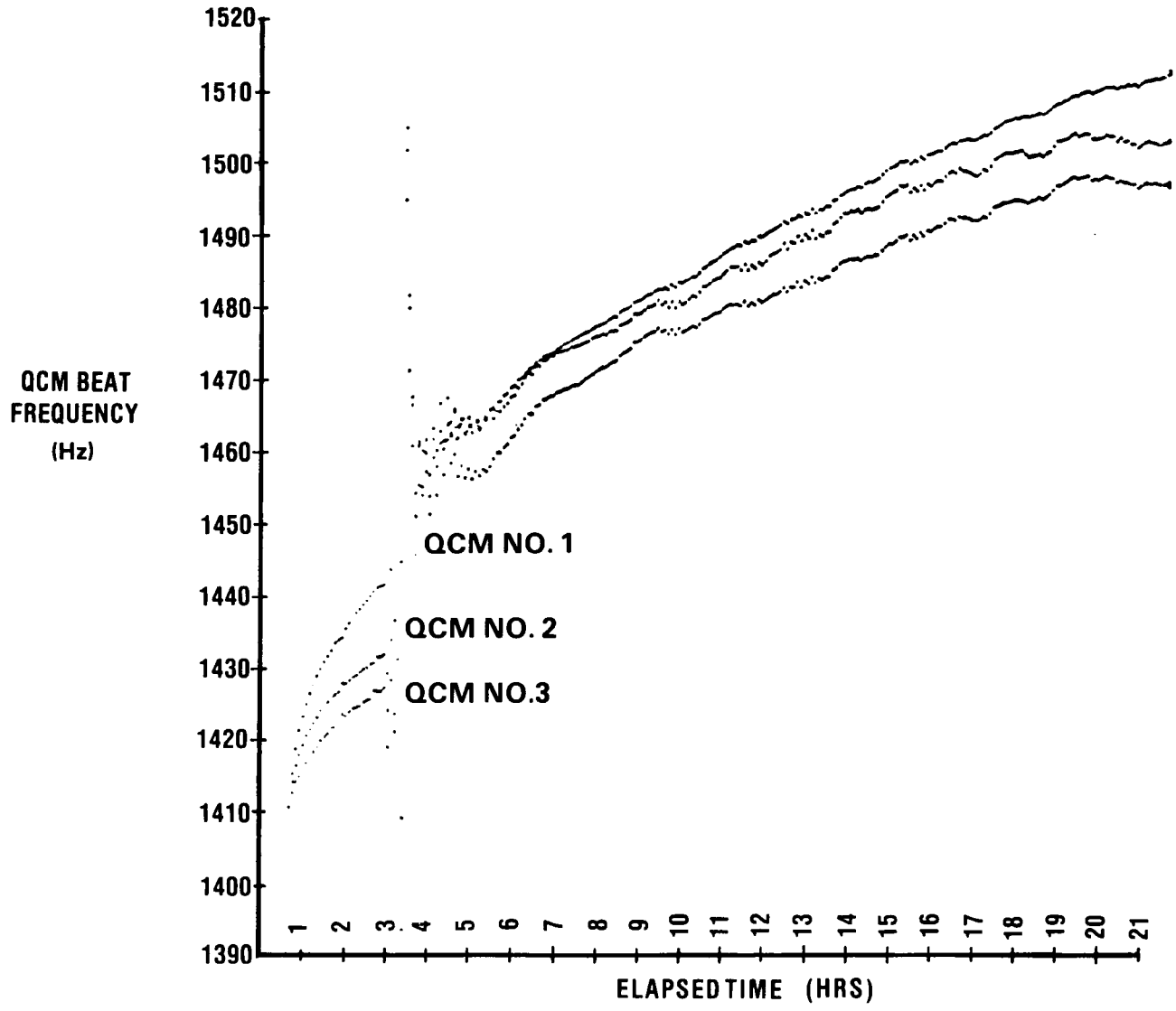

Figure 6. Isothermal QCM/TGA for DC 92-007 at a Temperature of 100°C

source emission is thus tentatively experimentally verified. Diffuse molecular reflection and VCM reemission, which are also fundamental assumptions of the model, have been experimentally determined in many other tests[1] so long as the surface is slightly contaminated and the temperature of incident molecular streams less than 700°C.

Using the "tail of the test" procedures for two 1st order components as outlined in previous subsections, the values of weight fractions and rate constants for DC 92-007 at 100°C were obtained. The weight fraction of 53% was taken from MMC TGA data and was presumed to include both the high and low volatiles. A high volatile weight fraction of 0.7% was obtained from the isothermal 100°C test with a rate constant of 1.75×10^{-3} per minute. The remaining 52.3% of the active low volatile had a rate constant of 4.24×10^{-6} per minute. Without a test at a second temperature, no estimate of activation energies or frequency factors was possible for these source components. This data, when compared with the test data point by point, gave poor correlation hence a diffusion model was tried assuming a single component.

This gave a considerably more satisfactory fit to the data than did the first order kinetics components. It is clear that due to the waviness of the data in the "tail" of this test unit DC 92-007 would be most difficult to analyze. No further reduction of data with this source was made.

At this point in the program, it was decided to continue detail kinetics testing on only one source material, RTV-566. Measurements of the isothermal outgassing kinetics for a 2.54 cm (1.0 inch) diameter coating of RTV-566 at four temperatures were made during this period. The temperatures were 40°C, 70°C, 100°C and 120°C. Data are presented in Figure 7 for these temperatures except for the 100°C run. A heater failure occurred during this test.

Additional information required are the physical dimensions of the sample coating itself. The procedures used are to peel the RTV

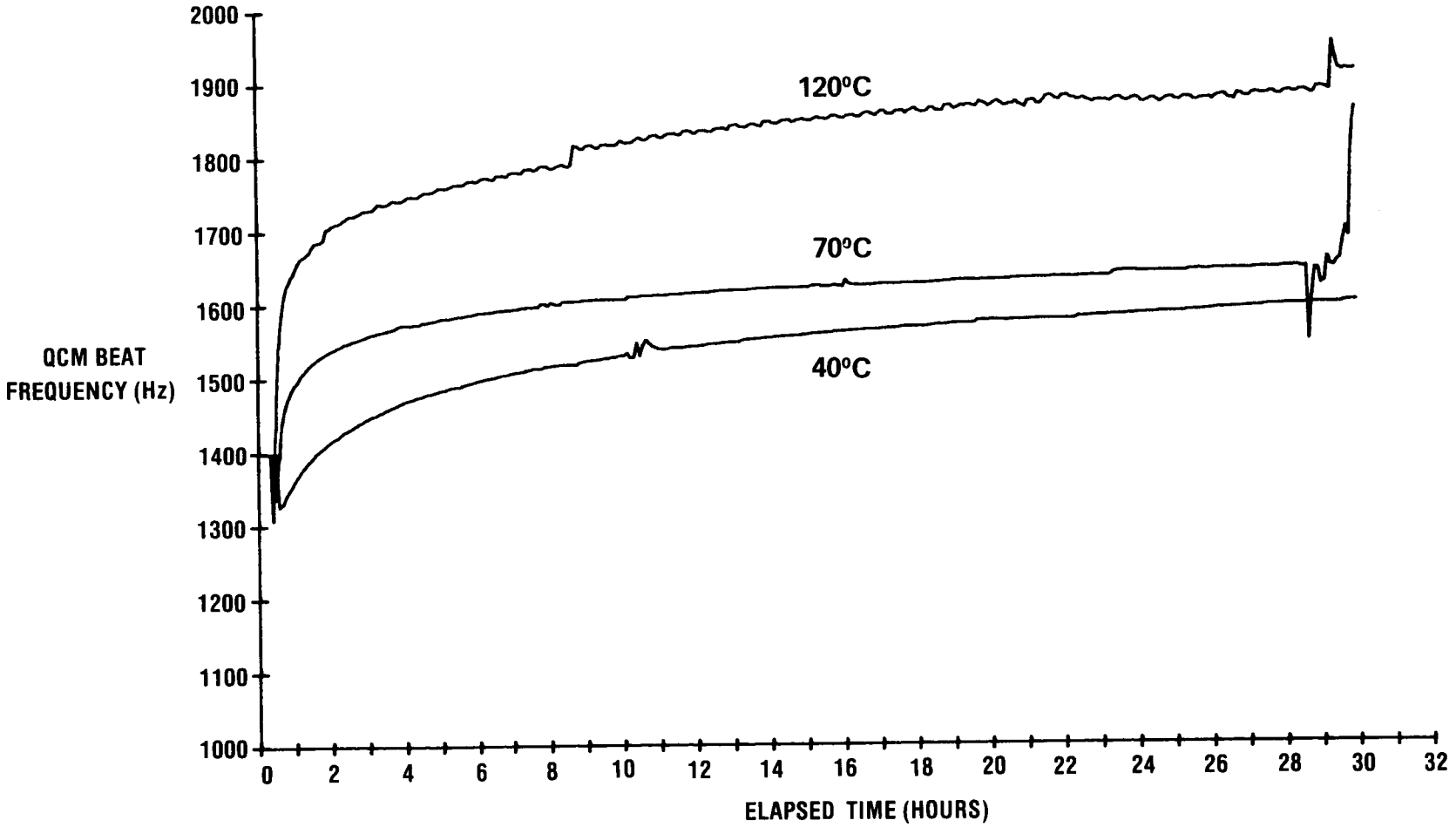

Figure 7. Isothermal QCM/TG Data for Three RTV-566 Coatings at 40, 70, and 120°C for Approximately 30 Hours Without UV Radiation

film away from the magnesium substrate after the test. Then, the resulting specimen is cut into a number of rectangular patches whose dimensions are easily measured. Each patch is then weighed to ±100 μg using an analytical balance. The thickness at various locations is measured, and the thickness measurements are averaged to obtain the reported value. A summary of these measurements for the four tests performed is given in Table I. A considerable variation in the thickness (±12 μm) is to be expected since the RTV-566 adhesive is applied with a spatula in a fairly viscous state following the vacuum degassing. However, the large variation in specific gravity is unusual. This has varied from about 0.90 (the samples readily float) up to 1.47. The manufacturer (G.E.) reports 1.51. This density variation is surprising in view of the fact that all the samples are from the same raw compounds of the same manufacturing process. The weight and thickness are necessary parameters in applying diffusion theory. As mentioned, the kinetics data for DC 92-007 at 100°C was quite satisfactorily modeled as a single diffusing process superimposed on a very low volatile single first order rate process.

TABLE I - RTV-566 TEST SAMPLE PHYSICAL PROPERTIES

Sample Number	Source Temp (°C)	Source Weight (mg)	Average Thickness (μm)	Source Area (cm^2)
27	40	45.1	69	5.067
28	70	47.9	109	5.067
*26	100	43.6	76	5.067
21	120	46.6	64	5.067

*Test deleted.

The basic nature of the RTV-566 and the measurement precision of the Molekit system necessitated the development of a relatively sophisticated data analysis algorithm to adequately reduce the QCM test data to obtain the desired source kinetic parameters.

A standard software package of polynomial regression and function analyzer routines was purchased from Hewlett Packard and these were linked together with the AESC plotter programs to be compatible with the data storage tapes. This system of programs, designated "POLYPLOT" (1) inputs the test data tapes and the QCM transient calibration, (2) fits a sequence of 9th order polynomials to the compensated QCM beat frequency data, (3) computes the derivatives of this function and (4) compares the regression analysis against the test data by plotting regression functions over the test data. The test data is therefore divided into a sequence of regression polynomials until the correlation coefficient is greater than 0.995. Then reliable slope and intercept determination from a log-linear plot of frequency rate versus time can be obtained. From these measurements, the kinetic parameters of the less volatile second component can be estimated, and subsequently the parameters for the first component evaluated by subtracting the effects of the second component from the test data at the start of the test when both components are active. With the assumption of first order kinetic processes for both components, the results of the data reduction are the percent by weight (weight fraction μ) of each component and the first order specific rate constant for each component (K). Table II presents this data at the three test source temperatures 40°C, 70°C and 120°C. Figure 8 shows the nearly linear dependency of the weight fraction of the high volatile component (μ_1) with source temperature. This could indicate an adsorbed material where the quantity that the surface will hold is inversely proportional to its temperature. The weight fraction of the second component can be averaged to give a value of about 0.21 ± 0.07. While the uncertainty is rather large, the average fraction

TABLE II. 1st ORDER SOURCE KINETICS DATA FOR TWO HIGH VOLATILE COMPONENTS OF RTV-566 (0.2% CATALYST)

TEMP T (°C)	WEIGHT W_S (mg)	DEPTH h (μm)	1st FRAC. μ_1 (%)	2nd FRAC. μ_2 (%)	1st RATE CONSTANT k_1 (MIN^{-1})	2nd RATE CONSTANT k_2 (MIN^{-1})
40	45.1	69	0.153	0.131	8.668×10^{-3}	9.330×10^{-4}
70	47.9	109	0.251	0.282	2.959×10^{-2}	9.493×10^{-5}
120	46.6	64	0.348	0.229	4.656×10^{-2}	2.007×10^{-3}

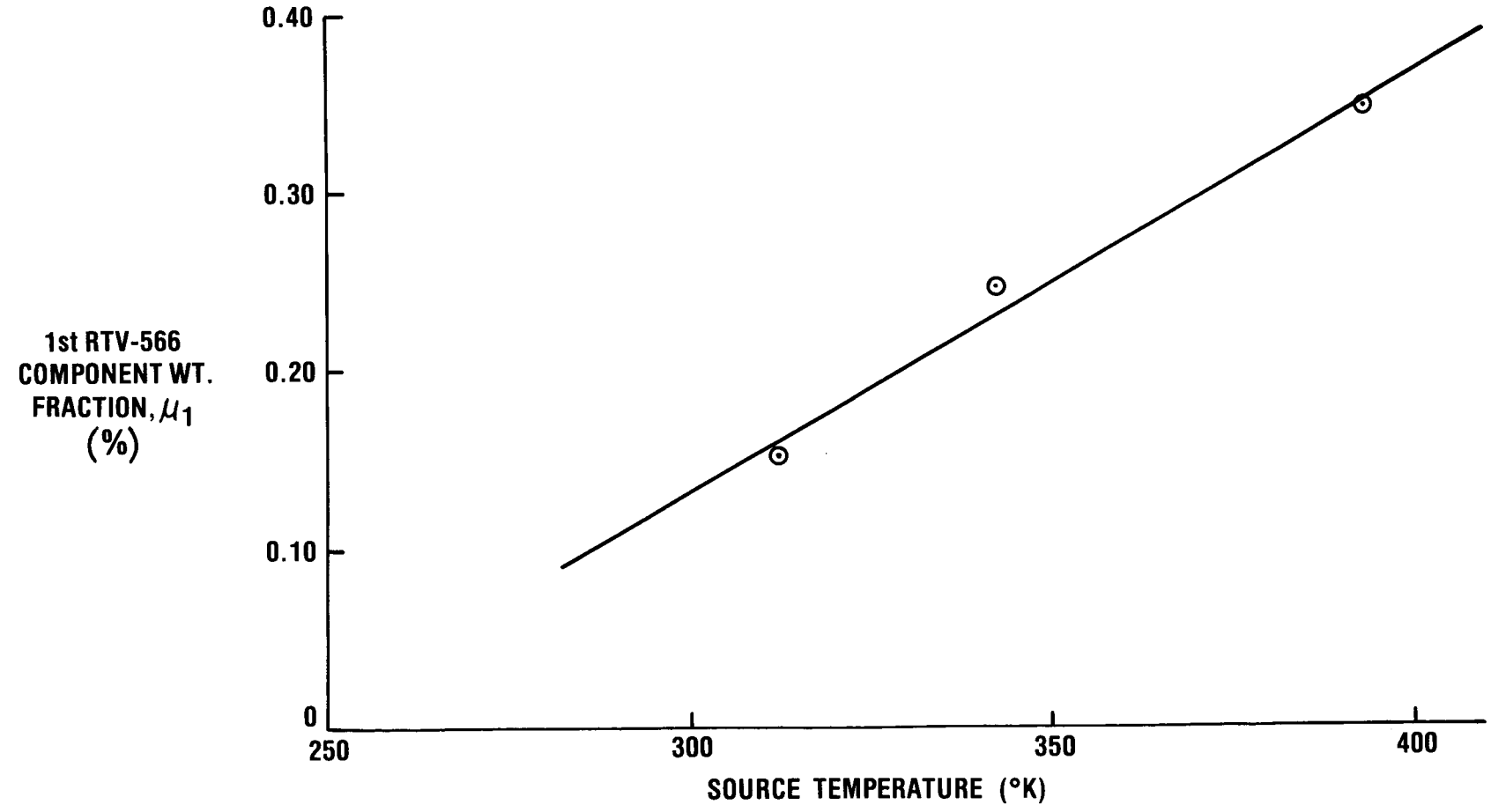

Figure 8. Variation of RTV-566 1st Component Wt. Fraction (%) with Source Temperature

of the second component which is released after twenty-four hours with the source at 120°C compares very closely with the NASA TND-8008 %TML of 0.23% for RTV-566 with 0.2% catalyst.

Figure 9 presents plot of the natural logarithm of the rate constants versus the reciprocal of the source temperature for both active components. The slope of such curves gives the value of the heat of activation for the process in question while the intercept at 1/T = 0 gives the so-called "frequency factor." The value of the rate constant at other temperatures can then be determined by using the Arrhenius relationship over the temperature range for which the slope is constant,

$$K(T) = A_o \, e^{-\Delta E/RT} \tag{6}$$

For the first component, a linear approximation with a correlation coefficient of 0.89 can be made showing

$$A_o^{(1)} = 32.15 \text{ min}^{-1}$$

$$\Delta E^{(1)} = 4990 \text{ cal mole}^{-1}.$$

For the second component, a linear relationship is not really indicated, but if it is assumed in spite of a very low correlation coefficient, then

$$A_o^{(2)} = 4.953 \times 10^{-1} \text{ min}^{-1}$$

$$\Delta E^{(2)} = 3083 \text{ cal mole}^{-1}.$$

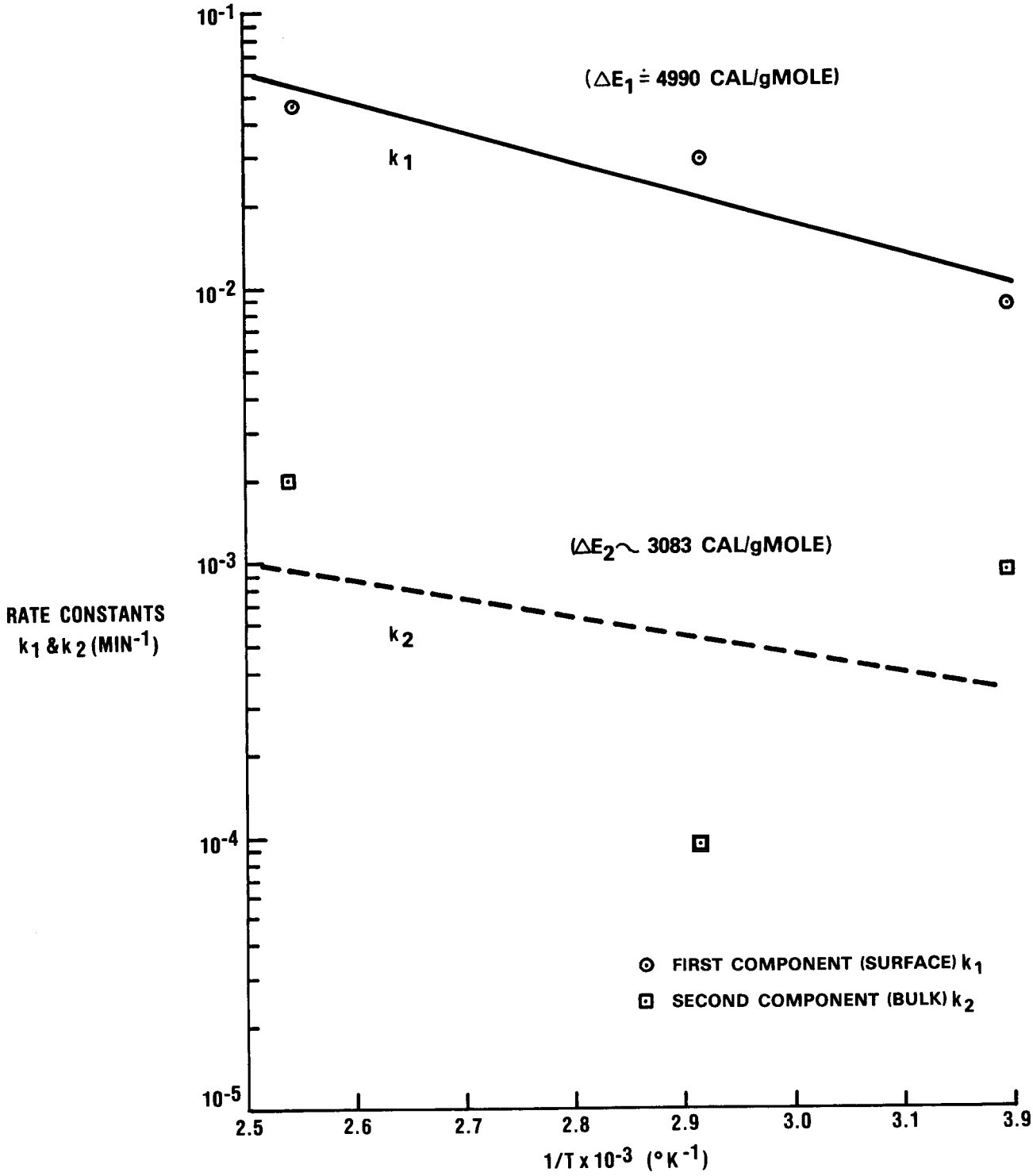

Figure 9. Rate Order Constants (Assuming First Order) of RTV-566 Versus Reciprocal Temperature for the Two High Volatile Components

For correlation as low as shown, it is equally valid to assume a constant value of rate constant over the temperature range; then

$$\Delta E^{(2)} = 0$$

$$9.5 \times 10^{-5} < \overline{K}_2(-1.01 \times 10^{-3}) < 2.01 \times 10^{-3} .$$

Typical calculations using the polynomial approximation for the source mass loss rate are shown in Figure 10 where the natural logarithm of the source mass loss rate $|\dot{M}_s|$ is plotted against the testing time. The typical decrease in the source rate by three orders of magnitude over the test period is clear. The absolute value (modulus) is shown since the real source mass loss rate is always a negative quantity.

2.5 VCM Reemission Test Procedures

This is a new technology in terms of systematic predictive model, thus a model was proposed based upon experience. Most pure substances exhibit a constant mass loss in vacuum.[3] This is classical evaporation and sublimation and is most frequently modeled using the Langmuir equation which expresses the mass loss rate per unit of surface area in terms of the bulk material temperature, mass number, and its equilibrium saturation vapor pressure. This well-known equation is

$$\dot{M}_s = \sqrt{\frac{M}{2\pi R T_s}}\, P_{sat}(T_s) \qquad (7)$$

where

$\dot{M}_s$ = Langmuir bulk reemission rate, g/cm^2 - s
M_s = VCM (a pure substance) atomic weight, AMU
R = universal gas constant, 1.986 cal/mole/^oK
T_s = bulk source temperature, ^oK

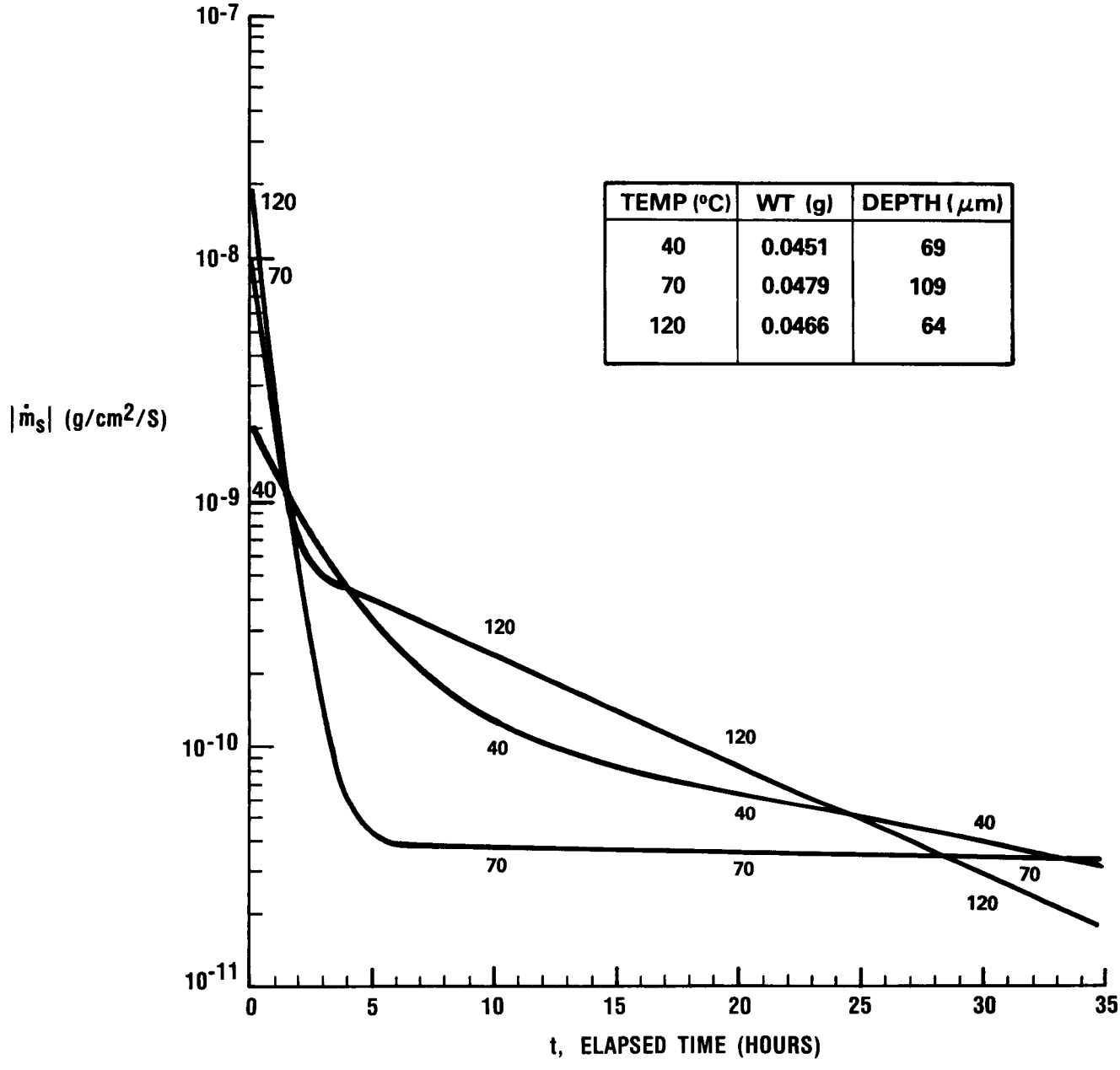

TEMP (°C)	WT (g)	DEPTH (μm)
40	0.0451	69
70	0.0479	109
120	0.0466	64

Figure 10. Mass Loss Rate for RTV-566 at 40, 70 and 120°C (0.2% Catalyst)

$P_{sat}(T_s)$ = equilibrium saturation vapor pressure at T_s, mm Hg(torr) .

In addition to this constant bulk reemission, recent tests have shown that small deposits reemit with an exponential time-dependency typical of a 1st order process[4], and it has been verified generally that surfaces covered with fractions of a monolayer exhibit 1st order reemission exactly[5] as for example the BET-Langmuir model of surface adsorption. In tests calibrating the precision of QCMs using a pure substance, ice, test data clearly showed that at least 1500 Å of ice had to exist on the receptor surface for a Langmuir constant reemission to occur[6]. The reemission rates decreased rapidly by several orders of magnitude as the coverage decreased to the very thin deposits of less than 500 Å which can then be modeled as 1st order processes.

Based upon this experimental evidence, the proposed AESC VCM reemission model assumes an exponential decrease in the reemission rate from the 1st order process at monolayer depths to the constant Langmuir rate when the surface is sufficiently covered to establish the bulk process. Typical of such processes at two receptor temperatures are sketched in Figure 11. The equation covers reemission kinetics ranging from a first order rate process for small receptor deposits to a constant mass loss reemission rate (zero order) for thick enough deposits that produce pure VCM bulk. This latter is identified with the Langmuir equation and is thus called a "Langmuir reemission process." With RTV-566, the basically high stability of the coating limits the outgassing to small values so that only small QCM deposits can be obtained, hence the small deposit first-order reemission kinetics is assured.

The test for the VCM reemission kinetics involves maintaining a clean QCM receptor at the temperature that the kinetics are to be evaluated. Then, the source is raised to a high temperature ($\approx 125^{\circ}C$), and the VCM allowed to deposit until a peak is reached, at which time the source is quenched with LN_2.

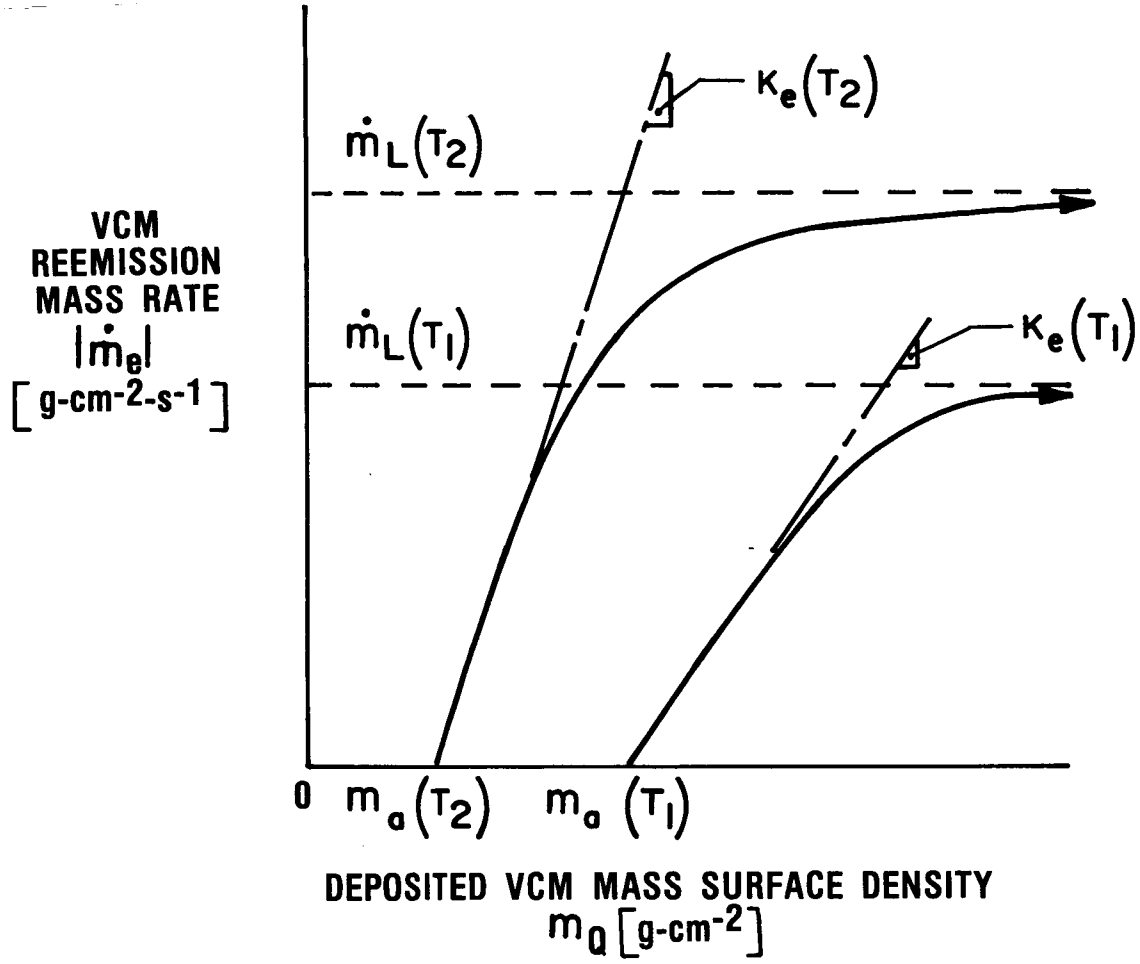

$$\dot{m}_e \doteq \dot{m}_L \left[1 - e^{\frac{K_e}{\dot{m}_L}(m_a - m_Q)} \right]$$

Figure 11. Schematic Diagram of VCM Reemission Mass Rate vs Deposited VCM Mass ($T_2 > T_1$)

The procedures for obtaining the VCM reemission rates constants for the two components can then be developed from the equation in Figure 11 for the QCM mass and mass rate equations assuming first order VCM reemission kinetics. The mass equation is

$$M_Q(t) = \sum_{i=1,2} \left[M_a^{(i)} \quad M_{QO}^{(i)} - M_a^{(i)} \; e^{-K_e^{(i)} t} \right] \tag{8}$$

where

$M_Q(t)$ = total mass on the QCM at time, g

$M_a^{(i)}$ = mass of i^{th} component which is permanently adsorbed onto the QCM, g

$M_{QO}^{(i)}$ = mass of the i^{th} component initially on the QCM immediately after quenching the source, g

$k_e^{(i)}$ = first order rate reemission rate constant for the i^{th} component, s^{-1}.

The mass rate equation for these two components is obtained by differentiating equation (8) to give

$$\dot{M}_Q = -\sum_{i=1,2} k_e^{(i)} \left[M_{QO}^{(i)} - M_a^{(i)} \right] e^{-K_e^{(i)} t} \tag{9}$$

As typical deposition test data shows, the HVC is rapidly reemitted so that in the "tail" (after eight hours), only the LVC is still actively being reemitted, and by plotting LN $|\dot{M}_Q|$ versus time in this domain, the rate constant $K_e^{(2)}$ and the mass differential $\left[M_{QO}^{(2)} - M_a^{(2)} \right]$ can be obtained from the slope and intercept respectively.

At the beginning of the reemission test, the QCM mass loss rate is given by

$$\dot{M}_Q(0) = -\sum_{i-1,2} k_e^{(i)}\left[M_{QO}^{(i)} - M_a^{(i)}\right] \tag{10}$$

Further, the total deposit on the QCM at the start and finish of the reemission test are respectively

$$\left.\begin{aligned} M_Q(0) &= \sum_i M_{QO}^{(i)} \\ M_Q(\infty) &= \sum_i M_a^{(i)} \end{aligned}\right\} \quad i = 1,2 \tag{11a, 11b}$$

By combining the data from the log-linear plot of $\dot{M}_Q$ versus t with equations (10) and (11), it is possible to evaluate the HVC rate constant

$$k_e^{(1)} = \frac{\left[M_Q(0)\right] - k_e^{(2)}\left[M_{QO}^{(2)} - M_a^{(2)}\right]}{\left[M_Q(0) - M_Q(\infty)\right] - \left[M_{QO}^{(2)} - M_a^{(2)}\right]} \tag{12}$$

2.6 VCM Reemission Test Results

Figure 12 shows a constant QCM mass loss rate at -20°C. It is a reasonable assumption that only the LVC is actively being reemitted and that its reemission rate constant is so small that a linear loss rate appears.

$$\dot{M}_Q = -k_e^{(2)}\left[M_{QO}^{(2)} - M_a^{(2)}\right] \tag{13}$$

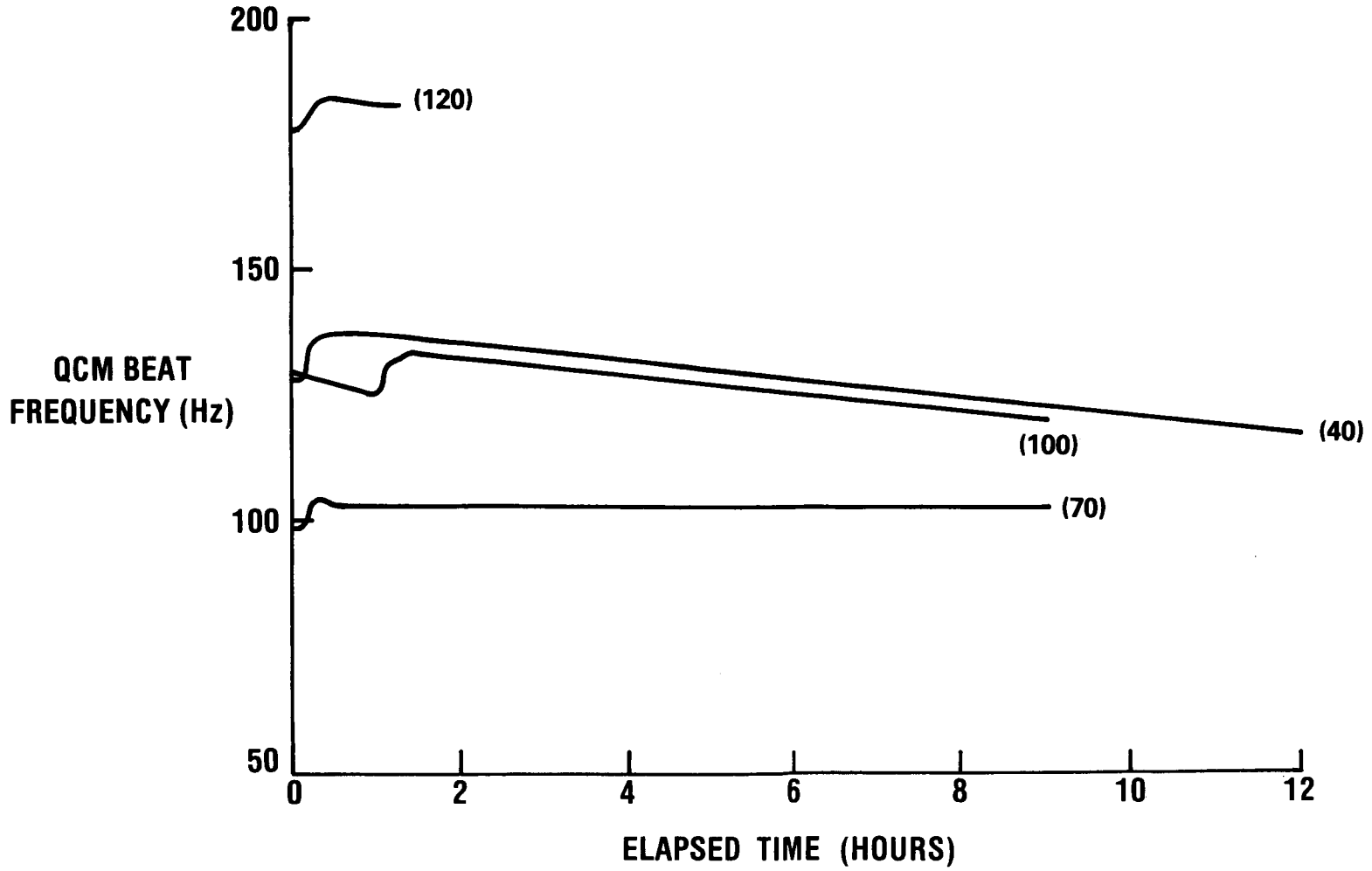

Figure 12. Reemission of Deposits from a QCM at -20°C After Termination of Deposition from RTV-566 at 40°, 70°, and 100°C

where

$$\dot{M}_Q = -2.115 \times 10^{12} \text{ g-s}^{-1}.$$

The initial quantity of LVC on the QCM, $M_{Q0}^{(2)}$, is obtained by extrapolating the constant reemission rate to the start of the test. The adsorbed quantity of the LVC, $M_a^{(2)}$, is assumed to be one-half of that shown in Figure 11.

For the QCM active crystal area of 0.316 cm^2, the mass surface density (MSD) becomes

$$m_a^{(2)}(-20^\circ C) = 1.82 \times 10^{-7} \text{ g-cm}^{-2}.$$

Assuming a VCM specific gravity of about 1.3, this gives deposit of LVC "thickness" of about 14 Å. The rate constant calculated for the LVC at $-20^\circ C$ is then

$$K_e^{(2)}(-20^\circ C) = 3.842 \times 10^{-4} \text{ min}^{-1} .$$

The reemission test for the source at $120^\circ C$ and the QCM at $10^\circ C$ showed an almost identical constant reemission about one hour after the HVC was emitted and by applying the same criteria as with the last case, the MSD

$$m_a^{(2)}(10^\circ C) = 1.557 \times 10^{-7} \text{ g-cm}^{-2}$$

which corresponds to a thickness of about 12 Å. The rate constant is

$$K_e^{(2)}(10^\circ C) = 9.311 \times 10^{4} \text{ min}^{-1} .$$

If classical ordered rate theory is assumed, then the LVC reemission rates will follow the Arrhenius relationship for temperature dependency. For the LVC data at $-20^{\circ}C$ and $10^{\circ}C$, these results are

$$K_e^{(2)} = A_o^{(2)} \, e^{\Delta Q^{(2)}/RT} \tag{14}$$

where

$A_o^{(2)}$ = 1.64 min^{-1}, the frequency factor for MVC reemission

$\Delta_Q^{(2)}$ = 4200 $cal\text{-}g^{-1}$ $mole^{-1}$, the heat of activation for MVC reemission.

The data for the reemission test at $10^{\circ}C$ had sufficient VCM at the start of the tests to permit the use of equations (11) and (12) to compute the rate constant of the HVC at $10^{\circ}C$.

$$K_e^{(1)}(10^{\circ}C) = 6.12 \times 10^{-2} \; min^{-1} \; .$$

All of the source and reemission processes of the two higher volatile components of RTV-566 studied with the isothermal QCM/TGA technique have exhibited low heats of activation characteristic of non-activated (physical) processes. In fact, they are all between 3000 and 5000 cal/g mole/$^{\circ}K$. It is probably safe to assume that the HVC reemission would show a similar heat of activation of about 4000 $cal\text{-}g^{-1}$ $mole^{-1}$. Then, the Arrhenius relation for the HVC becomes

$$K_e^{(1)} = A_o^{(1)} \, e^{\Delta Q^{(1)}/RT} \tag{15}$$

where

$A_o^{(1)} = 75.44\ min^{-1}$

$\Delta Q^{(1)} = 4000\ cal\text{-}g^{-1}\text{-}mole^{-1}$ (assumed).

Using this relationship, the HVC rate constant at ($-20^{\circ}C$) becomes

$$k_e^{(1)}(-20^{\circ}C) = 2.63 \times 10^{-2}\ min^{-1}.$$

The VCM reemission kinetics results are summarized in Table III. The first order kinetic model for VCM reemission is probably only valid for a limited thickness (about 150 Å was deposited in these tests). The reemission rate increases with the net deposited mass up to a maximum rate which is identified with the Knudsen-Langmuir loss rate ($\dot{m}_L$) classically related to the saturation vapor pressure. There is not enough VCM in the coated samples used in these tests to evaluate the Langmuir process.

2.7 Surface Transport Properties Test Procedures

This testing phase is primarily aimed at measuring the capture coefficients for VCM molecules emitting from the source at the source temperature, T_S, and impinging on the QCM receptor at T_Q. A temperature matrix of temperature combinations must be measured to account for the temperature range expected. The receptor temperatures were set at $-20^{\circ}C$, $+10^{\circ}C$ and $+25^{\circ}C$. Actually, above the $+10^{\circ}C$, almost no measurable deposit occurs. The source temperatures were the same as those used during the source kinetics testing.

The test procedures for these tests are obtained by integrating the QCM deposition differential equation which applies in the Molekit

TABLE III. REEMISSION KINETIC PROPERTIES FOR RTV-566 (0.2% CAT.)

QCM TEMP. °C	HIGH VOLATILE COMPONENT (HVC)		MEDIUM VOLATILE COMPONENT (MVC)	
	$A_o^{(1)} = 75.44\ MIN^{-1}$ $\Delta Q^{(1)} \cong 4.0\ KCAL/gMOLE$		$A_o^{(2)} = 1.64\ MIN^{-1}$ $\Delta Q^{(2)} = 4.2\ KCAL/gMOLE$	
	$m_a^{(1)}, \mu g\text{-}cm^{-2}$	$K_e^{(1)}, MIN^{-1}$	$m_a^{(2)}, \mu g\ cm^{-2}$	$K_e^{(2)}, MIN^{-1}$
-20	0.182	2.63×10^{-2}	0.182	3.84×10^{-4}
10	0.156	6.12×10^{-2}	0.156	9.31×10^{-4}

where the QCMs are at temperatures above LN_2. This expression is an extension of equation (1);

$$\dot{M}_Q + k_Q M_Q = -F_{SQ}\sigma_{SQ}\dot{M}_s \text{ g/s} \tag{16}$$

where

k_Q = VCM reemission rate constant from the QCM, s^{-1}

σ_{SQ} = capture coefficient for VCM molecules leaving the source at T_s and impinging on the QCM surface at T_Q.

Since first order kinetics has been applied to the two components of RTV-566 source, equation (16) can be integrated to give the desired Q/TGA equations. Then, to compute the two corresponding capture coefficients, it is necessary to examine the QCM mass and mass rate equations for the deposition transport tests. For the condition of a small deposit, 1st order source and VCM kinetics is assumed.

The QCM mass deposition equation for the two components is

$$M_Q = \sum_{i=1,2} M_a^{(i)} + F_{SQ}W_S\left[\frac{\sigma_{SQ}^{(i)}\mu^{(i)}k_s^{(i)}}{k_e^{(i)} - k_s^{(i)}}\right] x\text{---}$$

$$\text{---}x\left(e^{-k_s^{(i)}t} - e^{-k_e^{(i)}t}\right) \tag{17}$$

where

F_{SQ} = diffuse angle factor from the source to the QCM crystals

W_S = total source weight, g

$\sigma_{SQ}^{(i)}$ = capture coefficient of the i^{th} component arriving at the QCM from the source

$k_S^{(i)}$ = first order source rate constant for the i^{th} component, min^{-1} and

μ = weight factor of the i^{th} component in the source.

The QCM mass rate equation is obtained by differentiating equation (17) to give

$$\dot{M}_Q = \sum_{i=1,2} F_{SQ} W_S \left[\frac{\sigma_{SQ}^{(i)} \mu^{(i)} k_s^{(i)}}{k_e^{(i)} - k_s^{(i)}} \right] x---$$

$$---x \left(k_e^{(i)} \, e^{-k_e^{(i)} t} - k_s^{(i)} \, e^{-k_s^{(i)} t} \right) \qquad (18)$$

Allowing sufficient time ($\approx$ eight hours) to deplete the source of the high volatile component (HVC), equation (18), which is now an expression involving only the low volatile component (LVC), can be rearranged to determine the corresponding capture coefficient as follows:

$$\sigma_{SQ}^{(2)} = \frac{\left[k_e^{(2)} - k_S^{(2)} \dot{M}_Q(t) \right]}{\left(F_{SQ} \, \mu^{(2)} W_S k_S^{(2)} \right) \left(k_e^{(2)} \, e^{-k_e^{(2)} t} - k_S^{(2)} \, e^{-k_S^{(2)} t} \right)} \qquad (19)$$

at any value of $t \geq$ eight hours.

All the parameters on the right hand side of equation (19) are known from the source kinetics test and the reemission test. For good results, considering the typical difficulties with data reduction in analyzing "tail" data, several values of $\sigma_{SQ}^{(2)}$ at different times in the "tail" domain are calculated and the results averaged. Finally, the capture coefficient for the HVC can now be calculated using equation (18)

at any time during the initial hours of the transport test. The simplest result is the initial deposition, $\dot{M}_Q(0)$, rate which gives the following expression for the desired coefficient

$$\sigma_{SQ}^{(1)} = \frac{\dot{M}_Q(0) - F_{SQ}W_S\left[\sigma_{SQ}^{(2)}\ \mu^{(2)}\ K_S^{(2)}\right]}{F_{SQ}W_S\ \mu^{(1)}\ K_S^{(1)}} \tag{20}$$

Another convenient time at which to evaluate this coefficient is at the peak mass deposition when the mass rate vanishes. For many of the transport test conditions, this equilibrium point where the deposition rate vanishes is clearly evident and the elapsed time, t*, at which it occurs is easy to determine. When this occurs a particularly simple arrangement of the mass rate expressions allows simultaneous computation of both LVC and MVC capture coefficients knowing the initial QCM mass rate, $\dot{M}_Q(0)$, and the elapsed time at the peak deposition. Equations (18) and (20) can be combined into a matrix format as follows:

$$A_{ij}\ \sigma_{SQj} = B_i (i,j = 1,2) \tag{21}$$

where

σ_{SQj} = capture coefficient for i^{th} component of source onto the QCM

The elements of the coefficient matrix are given as follows:

$$A_{1,i} = \mu^{(i)}\ k_S^{(i)}\ (i = 1,2) \tag{22}$$

$$A_{2,i} = A_{1,i}\left\{\frac{k_e^{(i)}\ e^{-k_e^{(i)}t^*} - k_S^{(i)}\ e^{-k_S^{(i)}t^*}}{k_e^{(i)} - k_S^{(i)}}\right\} \tag{23}$$

$$B_1 = \left(\frac{\dot{M}_Q(0)}{F_{SQ} W_S} \right) \tag{24}$$

$$B_2 = 0 \ . \tag{25}$$

where

t^* = elapsed time at peak deposit, min and

$\dot{M}(0)$ = initial QCM mass accumulation, rate, g-min^{-1}

2.8 Surface Transport Properties Test Results

Transport deposit tests were made at QCM receptor temperatures of -20° and 10°C and at source temperatures of -40°C, 70°C, 100°C and 120°C. In addition, a single test was run with the source at 125°C and the QCM receptor at 25°C to compare Q/TGA testing results with those of the SRI-JPL TML/CVCM tests that are currently used to screen spacecraft materials.

The raw uncorrected QCM beat frequency data for the QCM at -20°C is presented in Figure 13. At the end of each deposition test, the source is quenched with LN_2. The QCM is maintained at -20°C and any subsequent VCM reemission measured. If there is still sufficient VCM in the QCM to make definitive reemission kinetics measurements, then this can be done. The data on VCM reemission kinetics of Figure 13 was taken after these transport deposition curves were made. At the QCM temperatures, no reemission was detected and separate reemission tests had to be performed.

Two general observations can be made based on the raw data. The first is that reemission rates exceed the incident flux rates, as is shown by the deposition peaks with the source at 70°C and 100°C. It also is true of the 120°C deposition curve, although it is not readily

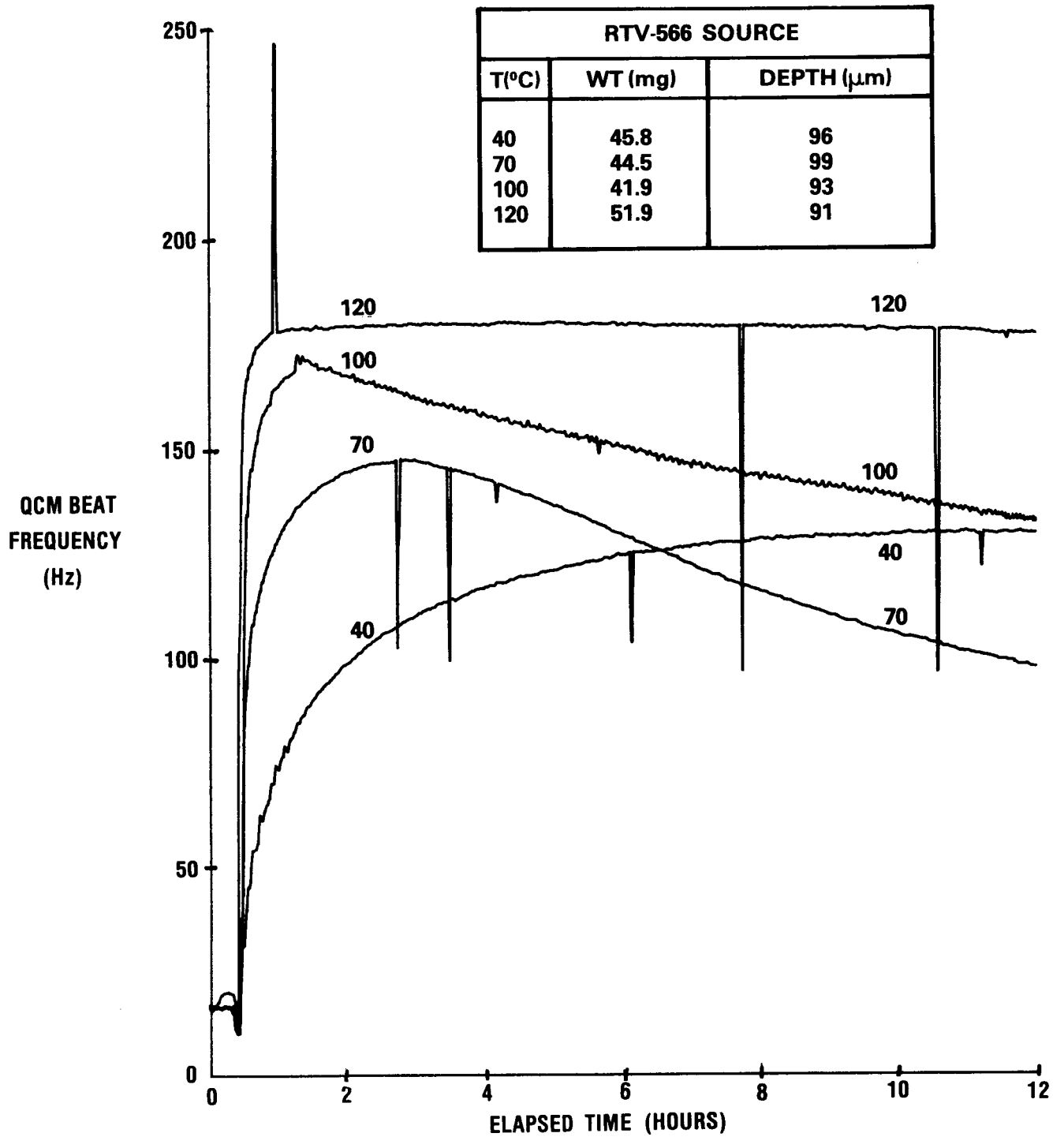

Figure 13. Deposition on a QCM at -20°C from RTV-566 (0.2% Cat.) Sources at 40°, 70°, 100° and 120°C

apparent on the plotting scale as shown. The second broad observation is that the residual amount of deposit is quite small.

If the specific gravity of the VCM is presumed to be about that of the RTV-566 resin or the catalyst, then the peak deposit from the source at 120°C corresponds to about 50 Å. It appears, therefore, that residual deposition may be limited to several adsorbed monolayers even when the source temperature is much greater than the receptor temperature. This also demonstrates the capability of Q/TGA techniques to measure depositions with monolayer precision.

The data for the transport deposition tests on the QCMs at +10° is presented in Figure 14. As with the -20°C test data, a "quick-look" examination shows two qualitative characteristics. One is the high VCM volatility and the other is a more or less permanently adsorbed residual deposit of about several monolayers. The initial mass deposit and deposit rate are noticeably greater than appeared in the source kinetics tests and the -20°C transport tests.

One cause for this increased mass release is that a new batch of RTV-566 source samples was made. While the identically same materials (resin and catalyst) were used and the manufacturing procedures rigorously followed, it is clear that the weight and thicknesses of the source specimens are from 50% to 150% greater than previous samples. The source data for the 10°C tests clearly shows the increase in the RTV-566 coating thickness. Hopefully, the intensive source kinetic properties (i.e., weight fractions and rate constants) will be invariant and only the additional source weight need be accounted for in reducing the data. However, to verify this will require additional source kinetics tests with this thicker batch of samples to compare with the previous data.

The transport test data for 10°C also indicates that after two to three hours, a permanently held residual VCM deposit is held on the QCM. This residual VCM (physisorbed) appears to depend upon the source

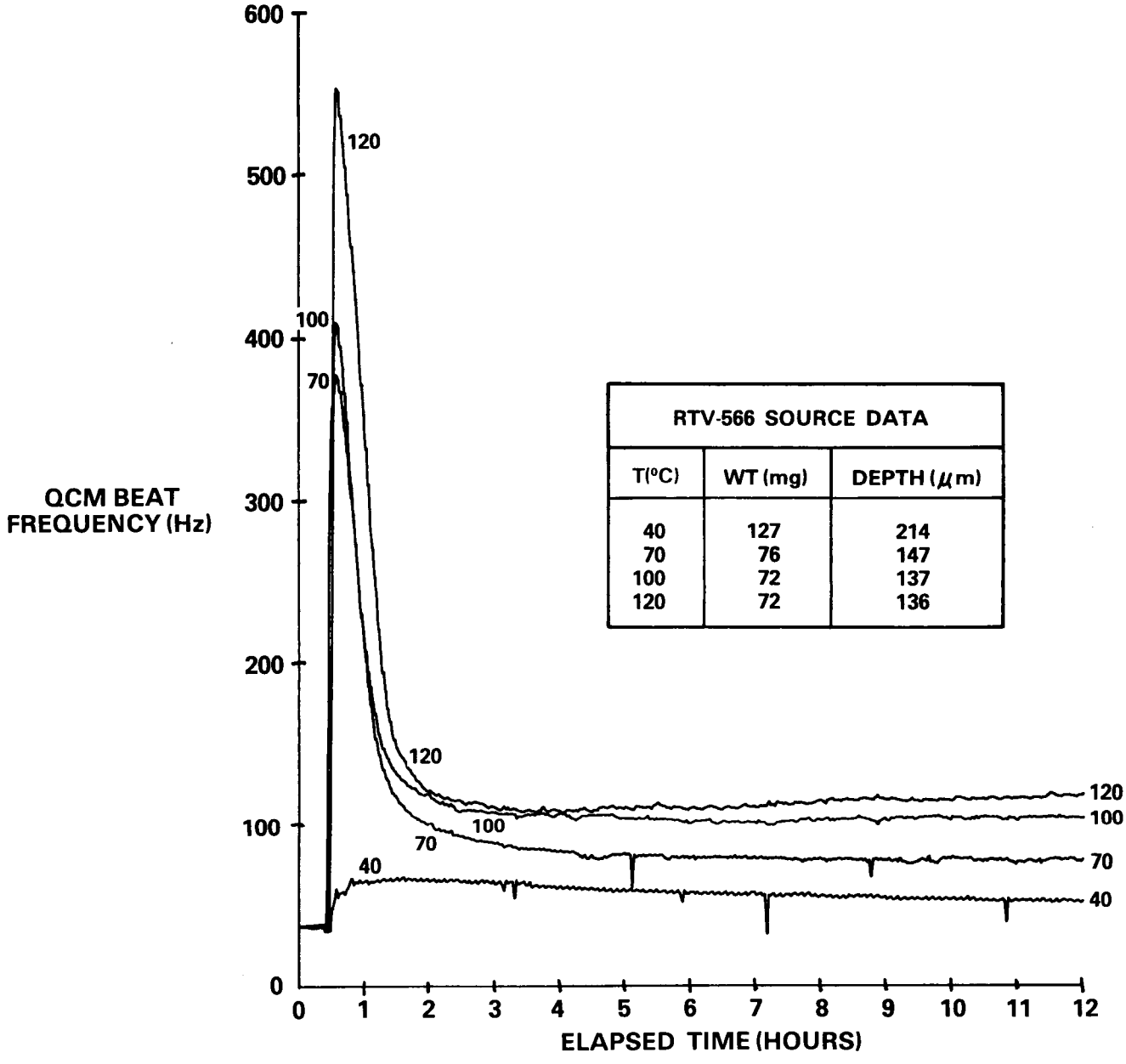

Figure 14. Deposition on a QCM at 10°C from RTV-566 (0.2% Cat.) Sources at 40°C, 70°C, 100°C and 120°C

temperature as the test data at the end of the test shows. An explanation of the variation of this final residual adsorbed deposit as a function of the source temperature will involve an in-depth analysis based on the physics of multilayer adsorption. This literature on adsorption under equilibrium conditions is plentiful, but there is very little covering the non-equilibrium conditions in these tests. For this reason, the relatively small residue is simply accounted for experimentally. However, the differences from equilibrium conditions indicate that a closer examination of these phenomena should be made.

Another special transport deposition test was run with the source at 125°C and the QCM at 25°C to investigate the relationships between the standardized JPL-SRI RML/CVCM data used to screen non-metallic materials for space application from a contamination potential viewpoint. Figure 15 shows these results with deposition transport data at -20°C and 10°C sketched in approximately to scale. In addition, the source kinetics test data for RTV-566 at 120°C when the QCM was maintained at -170°C is plotted. Thus, comparative deposition data at 4 QCM temperatures -170°C, -20°C, 10°C and 25°C is presented. The deposition amounts of the data curves for the QCM at -170°C and at 25°C after 24 hours of testing can be compared with the TML/CVCM data. The mass deposited on the cold QCM at point A measures the total mass lost by the source in twenty-four hours by knowing that the fraction of the released mass from the source which remains on the QCM is about 0.35% (diffuse) and that the total source mass is about 70 mg. The percent total mass loss (% TML) is then 0.3%. The QCM at -170°C is assumed to be totally anechoic and retains all the incident mass flux (i.e., $\dot{M}_e = 0$, $\sigma_{SQ} = 1.0$ for both components). When the QCM is maintained at 25°C, a slight transient deposit is desorbed in about one hour leaving the adsorbed deposit at point B, which is the percent collected volatile condensible mass (% CVCM) for both components. The ratio of the mass deposit at B to that at A shows that for the QCM at 25°C about 5% of that which hits

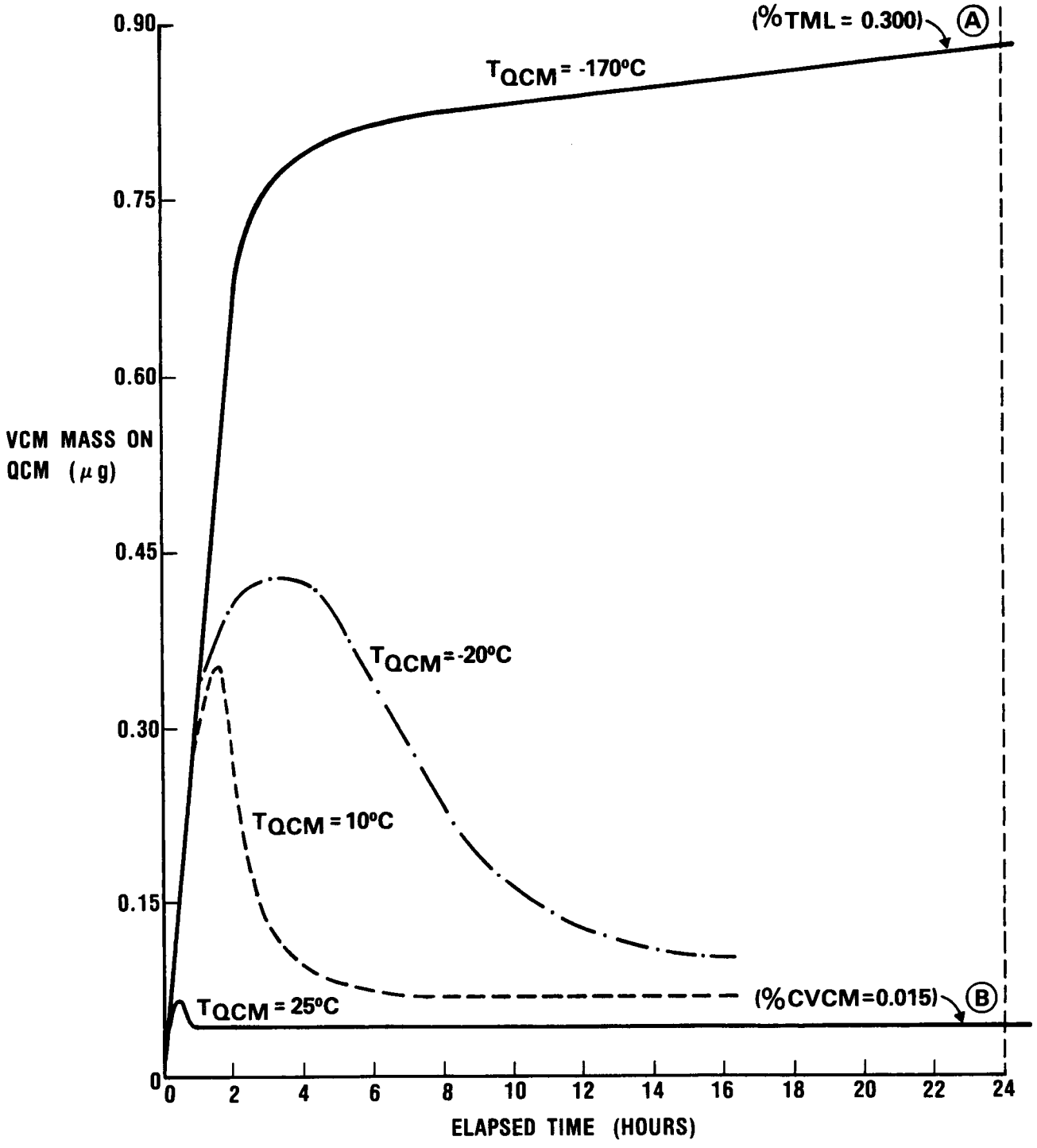

Figure 15. VCM Mass (μg) Deposited on a QCM Area 0.301 cm^2 Located 5.0 cm From a 2.54 cm. Dia. Source of RTV-566 (0.2% Cat.) Coated with 70 Mg and Maintained at 125°C for 24 Hrs.

the QCM collector is permanently adsorbed. The value gives 0.015% CVCM relative to the total source mass. The corresponding values published in Outgassing Data for Spacecraft Materials, NASA TN D-8008, gives for RTV-566 (0.2% catalyst) a % TML of 0.27% and a % CVCM less than 0.03%. Thus, these two isothermal QCM tests show the absolute relationships and transient nature of the data obtained from the JPL-SRI TML/CVCM measurements. Good correlation with the published TML/CVCM data was achieved.

It seems that the same TML/CVCM results could be obtained with five hours of testing instead of twenty-four hours. It also indicates that only about 10 Å to 15 Å of adsorbed VCM is retained on the collector.

Equations (21) and (22 - 25) can be applied to the four test conditions of the source at 120°C and 70°C and the QCM at -20°C and 10°C. The test conditions at 40°C must use the more general approach described, and no source kinetics data exists at 100°C. The results of these calculations are presented in Table IV. While the results must be considered preliminary pending a broader data base covering the variations in source mass and geometry, significant conclusions can be drawn from the results to date.

The capture coefficients for the QCMs at -170°C have been assumed to be 0.90. The correct physical assumption for a cryogenic receptor is not a unitary capture coefficient as might be expected but a negligible VCM reemission rate. The average value of the coefficients for all the transport measurements analyzed so far is about 0.92 to 0.04 which indicates a near uniform process occurring over the test temperature ranges tested. This shows a remarkable similarity to the classical Knudsen accommodation coefficient. This parameter is a measure of the probability that a molecule encountering a surface at a different temperature from the surface will attain the surface temperature. The incident molecule thus loses its previous identity, and becomes

TABLE IV. CAPTURE COEFFICIENTS FOR TWO COMPONENTS OF RTV-566 (0.2% CATALYST) FROM SOURCES AT (T_S) ONTO QCM RECEPTORS AT (T_Q)

T_S \ T_Q	-170°C		-20°C		10°C	
	$\sigma_{SQ}^{(1)}$	$\sigma_{SQ}^{(2)}$	$\sigma_{SQ}^{(1)}$	$\sigma_{SQ}^{(2)}$	$\sigma_{SQ}^{(1)}$	$\sigma_{SQ}^{(2)}$
40°C	(0.9) (ASSUMED)	(0.9)	DATA PROCESSING INCOMPLETE			
70°C	(0.9) (ASSUMED)	(0.9)	0.883	0.923	0.955	0.885
120°C	(0.9) (ASSUMED)	(0.9)	0.927	0.938	0.924	0.891

indistinguishable from other molecules of the same species on the surface. Recent studies in surface physical chemistry[5] show that this accommodation process requires but a few picoseconds in the case of physisorption.

Identifying the capture coefficient with the accommodation coefficient is completely consistent with the mass transport model as presently formulated when the VCM reemission is independently determined. The broad significance of a temperature-independent capture coefficient is that it is valid whether the incident molecules are hotter or colder than the receptor. A gravimetric measurement with a source colder than the receptor would probably be indeterminant since the reemission rates are signficantly higher than incident rates (viz, the deposition data greater than $10^{o}C$). Hopefully, for engineering applications with the ranges of temperatures under study, all capture coefficients can be assumed to be about 0.9. The only materials testing then required is to obtain the Arrhenius temperature relationships for the source VCM and its reemission; no matrix of coefficients need be determined.

These conclusions should be considered tentative until more data on other materials and conditions are obtained, but it does indicate a significant simplification in the analysis and testing of VCM transport properties.

3. RECEPTOR SURFACE EFFECTS TESTS

This section of the report covers the tests that were performed in the SMEF where the spectral reflectance change on 5 typical satellite receptor surfaces was measured. The classical Fresnel reflection equations for specular spectral reflection and transmission[8] require that a uniform thickness of film deposit exist on the substrate. To insure this, the mass transfer equations used in the previous section were employed to design the source holder and the carousel which supports the receptors to establish a uniform deposit within ±0.2%.

The spectral reflectance measurements were made on all 5 receptors in a Carey 14 monochromator in ambient laboratory conditions prior to placing these receptors in the SMEF. Then a similar ambient spectral measurement of reflectance was made using the optical system on the SMEF. By rationing these sets of measurements, the SMEF optics is calibrated at all wavelength measurements for absolute reflectance. Then, only changes in these values following the LN_2 quenching, the contamination deposition event, and the UV radiation are needed to obtain the desired effects.

The original test plan was to use a PbS detector at $-80^{\circ}C$ to make measurements from about 0.75 μm to 2.5 μm. However, this detector failed, and the spectral data was taken from 0.25 μm using a tungsten filament lamp. An S20 PMT was used as the detector with both lamps to cover the wavelength band from 0.25 μm to about 0.90 μm.

The measurements were completed following a deposition of 1000 Å from an RTV-566 source and a subsequent 36 hour exposure to 30 EUVS of ultraviolet irradiation at 1236 Å. However, considerable computer processing of the data is required to determine if a measurable change occurred since such a change will be very slight and "quick-look" study of the data isn't precise enough to indicate change.

3.1 AESC Surface Materials Effect Facility (SMEF)

The general specifications for the SMEF are similar to the Molekit except that the SMEF is a horizontal cylinder which is 1.22 m in diameter and 2.44 m long. The larger size permits the in-situ assembly of the more complex hardware required to make the effects measurements. The photograph of the SMEF in Figure 16 shows the overall configuration to be used to perform the hemispherical $\rho - \tau$ measurements. It consists of an integrating sphere system which includes a monochromator positioned outside and on top of the chamber with aspherical transfer optics to direct the light into the in-situ sphere.

The photograph in Figure 17 shows a closer view of the SMEF (with the loading door removed) with the receptor carousel rotated horizontally into the position where the deposition and UV irradiation occur. The 5 mounting locations for the 5 receptors on the carousel pinwheel are shown as well as the position of a QCM which is symmetrically positioned to have the same contamination depth as the receptors. Then the entire carousel, with the exception of the stepper motor which rotates the pinwheel, is cryogenically cooled and held at about $-160^{\circ}C$.

The final photograph in Figure 18 shows the carousel rotated into position in front of the integrating sphere following either a deposition or a UV radiation event.

The receptor pinwheel on the front end of the carousel can be indexed about the center line of the carousel through 360 degrees to position all the receptors in front of the sphere. The temperature of the source holder (not shown) and the carousel is maintained by precision controllers from $-160^{\circ}C$ to $130^{\circ}C$. The shroud is always at cryogenic temperature. The sphere components are typically at $-80^{\circ}C$. Fifteen thermocouples monitor temperatures throughout the SMEF.

The Hewlett-Packard 3050A data acquisition system which is coupled to both the Molekit and the SMEF automatically samples and records the photometric data. It has a capability to sample up to sixty

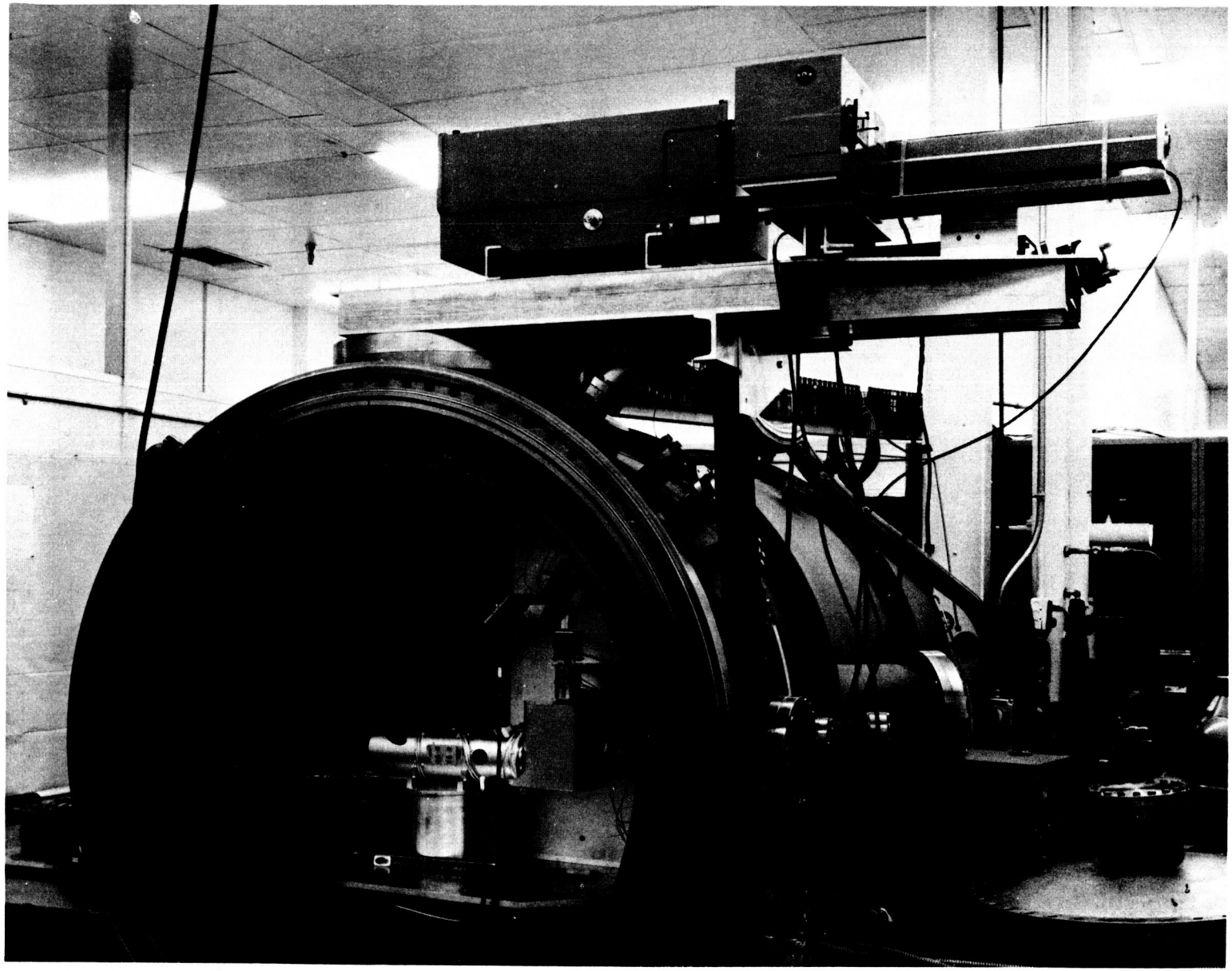

Figure 16. Surface Materials Effects Facility (SMEF) Configured for Spectral Reflectance/ Transmittance Measurements

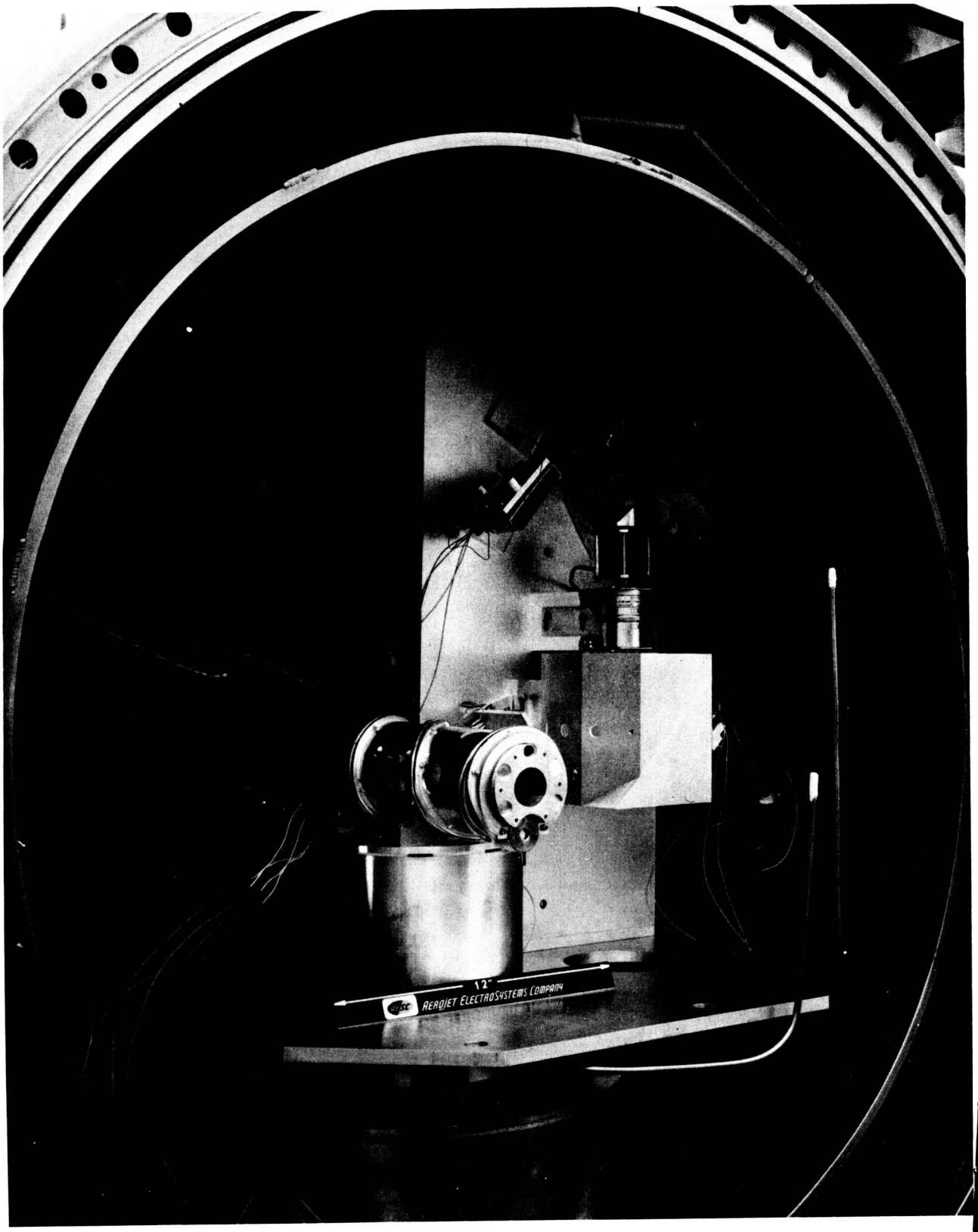

Figure 17. Sample Carousel Positioned for Deposition/Irradiation in SMEF

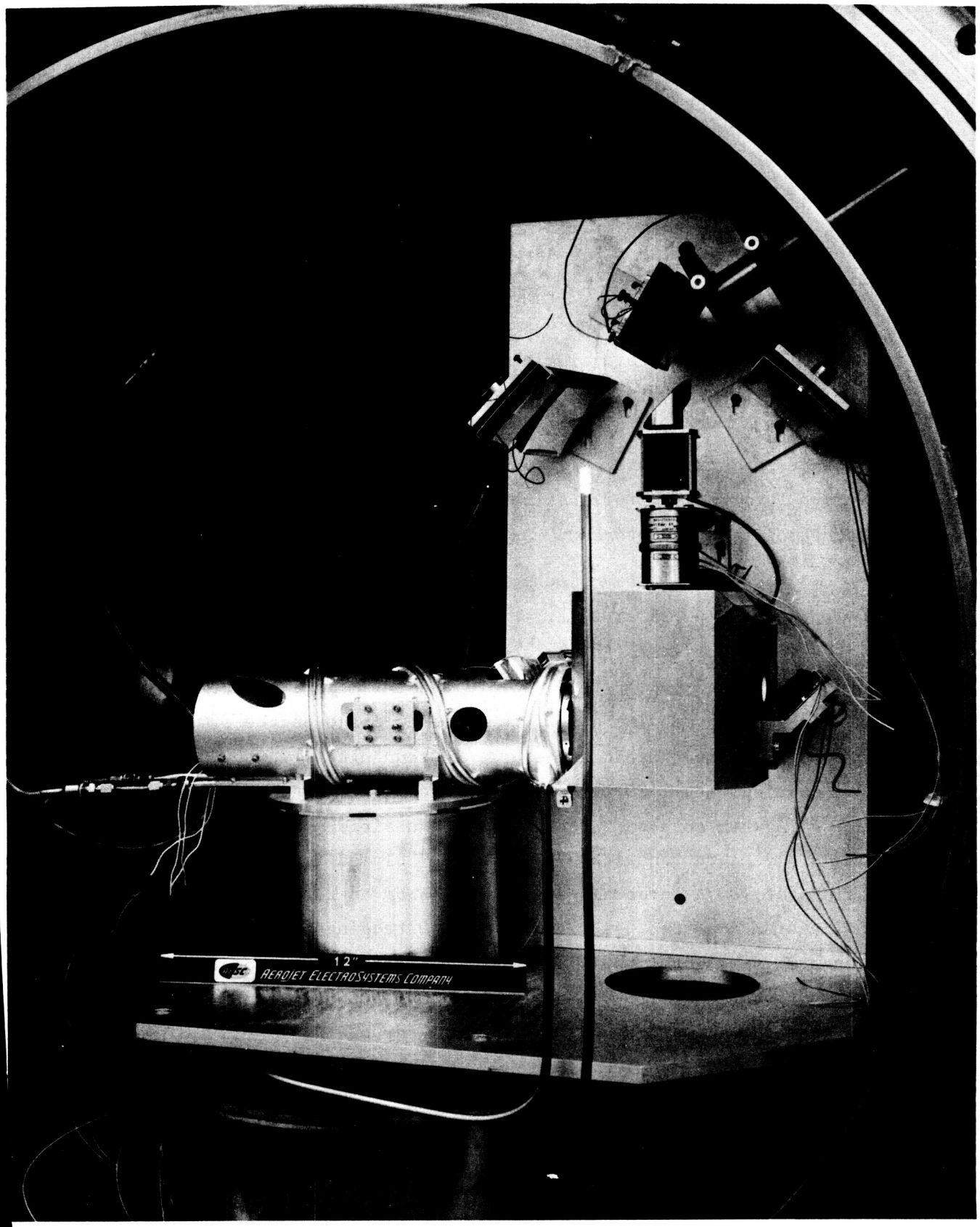

Figure 18. Sample Carousel Positioned for Effects Measurements in SMEF

channels of analog data with precision to 1 μV at a speed of about four channels per second. Data is stored on magnetic tape and can be simultaneously plotted and printed out as needed.

An optical schematic is shown in Figure 19 which traces the monochromatic light from the Jarral-Ash monochromator on top of the SMEF chamber into the chamber, through the integrating sphere and onto the desired receptor. To make a typical reflectance measurement, an oscillating rotatable scanning mirror is mounted in-situ on top of the integrating sphere which can provide a dual beam comparative photometric measurement of both reflectance and transmittance if desired. For the measurements made on this program, this mirror remained fixed in the position for spectral reflectance and the substitutional method of integrating sphere photometry was employed.

The Jarral-Ash monochromator can automatically scan the wavelengths from 0.25 μm to 2.5 μm at 500 Å min^{-1} so that values of the solar adsorptance can be calculated. Fixed circular slits 6 mm diameter are at the monochromator focal points and this image is put through the optical system producing a 1.25 cm diameter image on the sample part of the sphere. Three gratings are used in sequence. From 0.25 μm to 0.83 μm, a grating with 1180 lines·mm^{-1} blazed for 0.40 μm produces readings every 50 Å when coupled into the data acquisition system. From 0.83 μm to 1.46 μm, a grating with 590 lines·mm^{-1} blazed for 1.0 μm produces readings at 100 Å intervals and from 1.46 μm to 2.50 μm a grating with 295 lines·mm^{-1} blazed for 2.1 μm produces readings at 200 Å intervals. A tungsten filament lamp is used in conjunction with a photomultiplier tube (PMT) as a detector. The light beam is chopped at 200 Hz upon exit from the monochromator, and the PMT detector output is fed into a PAR lock-in amplifier. A dynamic range of five orders of magnitude is detectable. As with the Molekit, all data is automatically sampled and stored on tape.

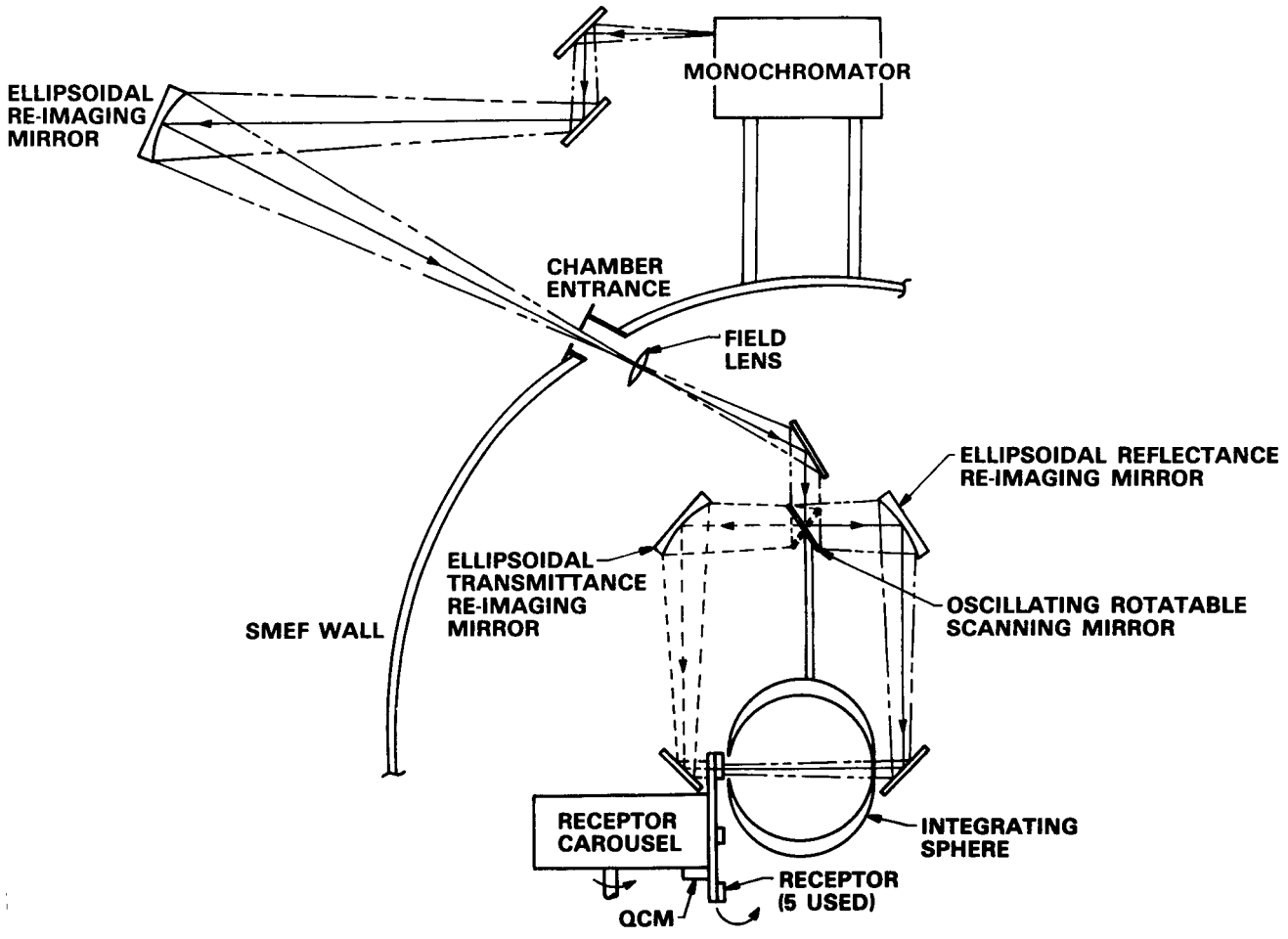

Figure 19. Optical Schematic of SMEF

3.2 Effects Measurements Procedures

In addition to the optical characteristics, there are some important procedural requirements in making the $\rho_\lambda - \tau_\lambda$ measurements. As with the Molekit, or any system which places the source material into vacuum, it is necessary to cool the source as quickly as possible as the pumpdown is started to minimize loss of the high volatile component. It is important to prevent icing on the source and QCM caused by LN_2 quenching of these components too early in the pumpdown sequence. It was found that in the SMEF the chamber pressure should be about 10^{-3} torr prior to quenching. This is essentially at the end of the roughing cycle after about thirty minutes of pumping. Thus the source is in vacuum about 30 minutes at ambient temperature at the start. This compares with 10 minutes in the Molekit. The maximum temperature that the double-ring source plate will reach in the SMEF is about $140^{\circ}C$ within 5 minutes from cryogenic equilibrium.

The carousel pinwheel which indexes the receptors across the sphere part supports 5 receptors. They are a gold first surface mirror which serves as the reference receptor (Au/REF) when using the substitutional method of sphere photometry. This reference mirror is shielded on the carousel to prevent contamination or UV irradiation. The remaining four receptors receive the full contamination-irradiation procedure. These receptors are (1) a gold first surface mirror (Au/FSM), (2) a sample of aluminized Teflon with 0.002 inches of Teflon mounted as a second surface mirror (AgFEP), (3) a 0.010 fused silica wafer coated with 1000 Å of silver mounted as a second surface mirror (Ag/SSM), and (4) a sample of S13GLO white paint 0.003" thick. All receptors are circular discs 1/2" in diameter. A QCM is positioned in the 6th pinwheel position (but doesn't index) and thus measures the VCM mass that is deposited on the four sample receptors. During the test period of about one week, the entire carousel is cryogenically cooled with LN_2 and thus all the attached components are held at about $-170^{\circ}C$.

An eight step procedure was used to evaluate the effects of UV irradiated contamination on the 4 sample receptors. First, the spectral reflectances of the Au/REF and the sample receptors were made ex-situ in a Carey 14 spectrophotometer. Second, reflectance measurements were made on each of the 5 receptors and of the baseline (no receptor at the sphere part) in the SMEF sphere system prior to evacuation and cooldown. This basically validates the basic performance of the SMEF sphere. Third, the SMEF chamber is evacuated and all internal components (carousel, source, shroud, sphere, optics, etc.) are quenched to LN_2 temperatures. Fourth, a reflectance measurement is again made on the clean, cool receptors. This measurement determines the optical path alignment distortion when the optical train is chilled to LN_2 temperatures. The optics are realigned as much as is possible for optimum measurements. Fifth, the carousel is positioned in front of the double-ring source, the source is quickly heated to about 135°C, and a deposition sequence takes place. About 1200 Å was deposited during these tests. Sixth, a measurement is then made of the contaminated but unirradiated receptors. The source is then quenched with LN_2. Seventh, the contaminated receptors are exposed to about 30 equivalent ultraviolet suns (30 EUVS) from a resonance electrodeless krypton lamp which emits radiation at 1236 Å for 36 hours. Eighth, a final reflectance measurement is made on the contaminated and irradiated receptors. This eight step procedure requires about one week with each measurement phase requiring about one working day. Most of the deposition and UV irradiation is performed overnight.

To calculate the spectral reflectance profile for a receptor using substitutional sphere photometry, the following equation is used

$$\rho_S(\lambda) = \left[\frac{I_S(\lambda) - I_B(\lambda)}{I_R(\lambda) - I_B(\lambda)}\right] \rho_R(\lambda) \qquad (26)$$

where

$\rho_S(\lambda)$ = hemispherical spectral reflectance of a sample receptor at λ

$\rho_R(\lambda)$ = hemispherical spectral reflectance of the reference receptor (Au/REF) at λ

$I_S(\lambda)$ = photomultiplier current of sphere detector when the sample is being illuminated, milliamps

$I_R(\lambda)$ = PMT current of sphere detector when the reflectance receptor is being illuminated, milliamps

$I_B(\lambda)$ = PMT current for the baseline measurement where no receptor covers the sphere port, milliamps

Thus, six scans through the wavelength range from 0.25 μm to 2.5 μm is required during each measurement phase. Each receptor is sampled at 250 wavelengths. A total of 1500 data points are stored on tape. To compute the profiles using equation (26), a computer is required. At present the software programs to completely perform these calculations and plot the reflectance profiles have just been completed and only "spot" checks of the data are available.

References

1. Nocilla, S. "The Surface Reemission Law in Free Molecule Flow" Rarefied Gas Dynamics, Supp. 2, Vol. 1, p. 327, Academic Press, 1963

2. Whipple, C. L. and Thorne, J. A. "Silicones in Outer Space" The Effects of Space Environment on Materials, Vol. II, p. 243, Proceedings of the 11th National Symposium and Exhibit of the Society of Aerospace Materials and Process Engineers (SAMPE), St. Louis, 1967

3. Buckley, P. H. and Johnson, R. L. "Evaporation Rates for Various Organic Liquid and Solid Lubricants in Vacuum to 10^{-8} mm Hg at 55°F to 1100°F", NASA TN D-2081, National Aeronautics and Space Administration, Washington, D.C., December 1963

4. "Investigation of Contamination Effects on Thermal Control Materials", AFML-TR-74-218, Final Technical Report, AFML/MBE, Wright-Patterson Air Force Base, Ohio, June 1974

5. Adamson, A. W. Physical Chemistry of Surfaces, Jim Wiley and Sons, 3rd Ed. 1976

6. Glassford, A. P. M. "An Analysis of the Accuracy of a Commercial Quartz Crystal Microbalance", Paper No. 76-438 presented at the 11th AIAA Thermophysics Conference, San Diego, Cal., July, 1976

7. Glasstone, S., Laidlor, K., and Eyring, H., The Theory of Rate Processes, McGraw-Hill Book Co., Inc., 1st Edition, 4th Impression, 1941

8. Born, M. and Wolf, E., Principles of Optics, 3rd Ed. (Rev.) Pereamon Press, N.Y., 1965